Interactions, superconducting T_c, and fluctuation magnetization for two coupled dots in the crossover between the Gaussian Orthogonal and Unitary ensembles

Oleksandr Zelyak* and Ganpathy Murthy†

Department of Physics and Astronomy,

University of Kentucky, Lexington, Kentucky 40506, USA

Igor Rozhkov‡

Department of Physics, University of Dayton,

300 College Park, Dayton, OH 45469

(Dated: February 1, 2008)

Abstract

We study a system of two quantum dots connected by a hopping bridge. Both the dots and connecting region are assumed to be in universal crossover regimes between Gaussian Orthogonal and Unitary ensembles. Using a diagrammatic approach appropriate for energy separations much larger than the level spacing we obtain the ensemble-averaged one- and two-particle Green's functions. It turns out that the diffuson and cooperon parts of the two-particle Green's function can be described by separate scaling functions. We then use this information to investigate a model interacting system in which one dot has an attractive s-wave reduced Bardeen-Cooper-Schrieffer interaction, while the other is noninteracting but subject to an orbital magnetic field. We find that the critical temperature is *nonmonotonic* in the flux through the second dot in a certain regime of interdot coupling. Likewise, the fluctuation magnetization above the critical temperature is also nonmonotonic in this regime, can be either diamagnetic or paramagnetic, and can be deduced from the cooperon scaling function.

PACS numbers: 73.21.La, 05.40.-a, 73.50.Jt

Keywords: quantum dot, scaling function, crossover, quantum criticality

I. INTRODUCTION

The idea of describing a physical system by a random matrix Hamiltonian to explain its spectral properties goes back to Wigner[1,2]. It was further developed by Dyson, Mehta and others, and became the basis for Random Matrix Theory (RMT)[3]. First introduced in nuclear physics, RMT has been used with great success in other branches of physics and mathematics. A notable example was a conjecture by Gorkov and Eliashberg[4] that the single-particle spectrum of a diffusive metallic grain is controlled by RMT. This conjecture was proved by Altshuler and Shklovskii[5] who used diagrammatic methods and by Efetov who used the supersymmetry method[6]. In 1984 Bohigas, Giannoni and Schmit[7] conjectured that RMT could also be employed in the study of ballistic quantum systems whose dynamics is chaotic in the classical limit. Their conjecture broadened the area of applicability of RMT enormously and was supported by numerous ensuing experiments and numerical simulations[7,8,9,10]. The crucial energy scale for the applicability of RMT is the Thouless energy $E_T = \hbar/\tau_{erg}$, where τ_{erg} is the time for a wave packet to spread over the entire system. For a diffusive system of size L, we have $E_T \simeq \hbar D/L^2$, while for a ballistic/chaotic system we have $E_T \simeq \hbar v_F/L$, where v_F is the Fermi velocity.

In this paper we consider a system of two quantum dots/nanoparticles which are coupled by a hopping bridge. The motion of electrons inside each dot can be either ballistic or diffusive. In the case of ballistic dots we assume that the dots have irregular shapes leading to classically chaotic motion, so that RMT is applicable.

RMT Hamiltonians fall into three main ensembles[3]. These are the Gaussian Orthogonal Ensemble (GOE), Gaussian Unitary Ensemble (GUE), and Gaussian Symplectic Ensemble (GSE). They are classified according to their properties time-reversal (TR). The Hamiltonians invariant with respect to TR belong to the GOE. An example of GOE is a quantum dot which has no spin-orbit coupling and is not subject to an external magnetic field. GUE Hamiltonians, on the contrary, are not invariant with respect to TR and describe motion in an orbital magnetic field, with or without spin-orbit coupling. Hamiltonians from GSE group describe systems of particles with Kramers degeneracy that are TR invariant but have no spatial symmetries, and correspond to systems with spin-orbit coupling but with no orbital magnetic flux. In our paper we only deal with the first two classes.

For weak magnetic flux the spectral properties of the system deviate from those predicted

by either the GOE or the GUE[11]. In such cases the system is said to be in a crossover[3]. For these systems the Hamiltonian can be decomposed into real symmetric and real antisymmetric matrices:

$$H = \frac{H_S + iXH_A}{\sqrt{1+X^2}}, \tag{1}$$

where X is the crossover parameter[12] which is equal, up to factors of order unity, to Φ/Φ_0, where Φ is the magnetic flux through the dot, and $\Phi_0 = h/e$ is the quantum unit of magnetic flux. Note that the gaussian orthogonal and unitary ensembles are limiting cases of $X \to 0$ and $X \to 1$ respectively.

To understand the meaning of the crossover parameter consider the Aharonov-Bohm phase shift picked up by a ballistic electron in a single orbit in the dot:

$$\Delta\phi = 2\pi\frac{\Phi}{\Phi_0}. \tag{2}$$

For one turn the flux enclosed by the trajectory is proportional to $\Phi = BL^2$, where L is the size of the dot. After N turns the total flux is $\Phi_{total} = \sqrt{N}\Phi$, where factor $\sqrt{N}$ originates from the fact that electron has equal probability to make clockwise or counterclockwise orbits, and thus does a random walk in the total flux enclosed. The minimal phase shift for the electron to notice the presence of the magnetic flux is of the order 2π, and thus the minimal cumulative flux enclosed by the orbit should be $\Phi_0 = \sqrt{N}\Phi$. This leads to $N = (\Phi_0/\Phi)^2$, while the time to make N turns is $\tau = LN/v_f$ (for a ballistic/chaotic dot). From the Heisenberg uncertainty principle the associated energy scale is:

$$E_{cross} \approx \frac{\hbar}{\tau} = \frac{E_T}{N} = E_T\left(\frac{\Phi}{\Phi_0}\right)^2, \tag{3}$$

where E_T is the ballistic Thouless energy[13]. For a diffusive dot it should be substituted by the diffusive Thouless energy $E_T \cong \hbar D/L^2$. One can see that when Φ is equal to Φ_0, E_X is equal to E_T which means that energy levels are fully crossed over.

In this paper the reader will encounter many crossover parameters, and thus many crossover energy scales. By a line of argument similar to that leading to Eq. (3), it can be shown that to every crossover parameter X_i there is a corresponding energy scale $E_{X_i} \simeq X_i^2 E_T$.

Breaking the time reversal symmetry of system changes the two-particle Green's function. While the two-particle Green's function can in general depend separately on E_T, E_X, and the measurement frequency ω, it turns out that in the universal limit $\omega,\ E_X \ll E_T$, it becomes a *universal scaling function* of the ratio E_X/ω. The scaling function describes the modification of $\langle G^R(E+\omega)G^A(E)\rangle$ as one moves away from the "critical" point $\omega = 0$. The limits of the scaling function can be understood as follows: If the measurement frequency ω is large (small) compared to the crossover energy scale E_X, the $\langle G^R(E+\omega)G^A(E)\rangle$ takes the form of the GOE (GUE) ensemble correlation function. If $\omega \sim E_X$, the Green's function describes the system in crossover regime.

The one-particle Green's function $\langle G^R(E)\rangle$ is not critical as $\omega \to 0$, although it gets modified by the interdot coupling. The two-particle Green's function $\langle G^R(E+\omega)G^A(E)\rangle$ always has a diffuson mode[14], that diverges for small ω in our large-N approximation, which means that our results are valid on scales much larger than mean level spacing. This divergence is not physical and will be cut off by vanishing level correlations for $\omega \ll \delta$ in a more exact calculation[15]. On the other hand, the energy scale ω should be smaller than Thouless energy of the system for RMT to be applicable. These limitations hold for the crossover energy E_X as well. In what follows we study the regime corresponding to $\delta \ll \omega, E_X \leq E_T$.

The other term that appears in the two-particle Green's function is a cooperon mode. In general the cooperon term is gapped if at least one of the crossover parameters is different from zero. In the case when the total Hamiltonian of the system is time reversal invariant, all the crossover parameters are zero and the cooperon, just like the diffuson, becomes gapless. Finally, when each part of compound system belongs to the GUE (the case when all crossover parameters are much larger than ω) the cooperon term disappears.

Our study has a two-fold motivation. The first part comes from works on coupled structures with noninteracting particles in acoustic and electronic systems[16,17,18], and crossovers[11,19,20,21,22]. We focus on a complete description of the crossover regimes in all three regions (the two dots and the bridge) and define scaling functions for the diffuson and cooperon parts of the two-particle Green's function. Using parameters analogous to E_X we describe crossover regimes in dots 1 and 2 and the effects of the tunable hopping between them. Varying these parameters allows us to obtain results for various physical realizations, when different parts of the compound system behave as pure GOE, GUE, or belong to the

crossover ensemble. In electronic systems it is easy to break time-reversal by turning on an external orbital magnetic flux. In acoustic systems one can break time-reversal by rotating the system or a part thereof. As mentioned before, the system of two dots coupled by hopping has been investigated before using supersymmetry methods[18]. However, the authors considered only the GUE, whereas here we are interested in the full crossover. In fact, the crossover is essential to the second aspect of our work, as will become clear immediately.

The second part of our motivation is the possibility of using the information gained in noninteracting systems to predict the behavior of interacting systems[23,24,25,26]. We consider interacting systems controlled by the Universal Hamiltonian[27,28,29,30], which is known to be the interacting low-energy effective theory[31,32,33] deep within the Thouless band $|\varepsilon - \varepsilon_F| \ll E_T$ in the renormalization group[34,35] sense for weak-coupling when the kinetic energy is described by RMT and the Thouless number $g = E_T/\delta \gg 1$. For the GOE the Universal Hamiltonian H_U has the form[27,28,29,30]

$$H_U = \sum_{\alpha,s} \epsilon_\alpha c^\dagger_{\alpha,s} c_{\alpha,s} + \frac{U_0}{2}\hat{N}^2 - J\mathbf{S}^2 + \lambda T^\dagger T \tag{4}$$

where $\hat{N}$ is the total particle number, $\mathbf{S}$ is the total spin, and $T = \sum c_{\beta,\downarrow} c_{\beta,\uparrow}$. In addition to the charging energy, H_U has a Stoner exchange energy J and a reduced superconducting coupling λ. This last term is absent in the GUE, while the exchange term disappears in the GSE.

In this paper we concentrate on the reduced Bardeen-Cooper-Schrieffer (BCS) coupling λ which leads to a mean-field superconducting state when $\lambda < 0$. Previous work by one of us[26] sets the context for our investigation. We consider an interacting system which has a single-particle symmetry and a quantum phase transition in the limit $E_T/\delta \to \infty$. An example relevant to us is a superconducting nanoparticle originally in the GOE. It has the reduced BCS interaction and time-reversal symmetry, and the (mean-field) quantum phase transition is between the normal and superconducting states and occurs at $\lambda = 0$. Now consider the situation when the symmetry is softly broken, so that the single-particle dynamics is described by a crossover RMT ensemble. It can be shown[26] that this step allows us to tune into the *many-body quantum critical regime*[36,37,38] of the interacting system. Thus, the scaling functions of the noninteracting crossover are transmuted into scaling functions of the interacting system in the many-body quantum critical regime. In our example, the orbital magnetic flux breaks the time-reversal symmetry which is crucial to superconductivity.

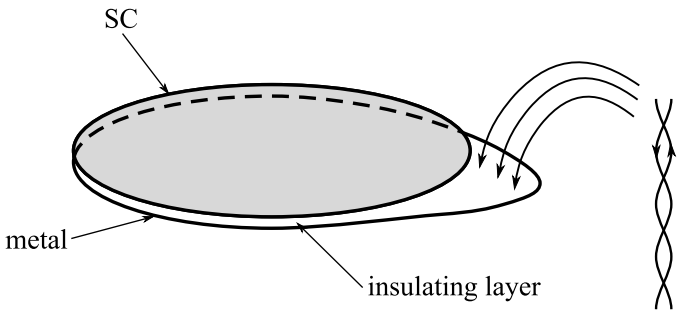

FIG. 1: The system of two vertically coupled quantum dots.

When the orbital flux increases to a critical value, it destroys the mean-field superconducting state. Above the critical field, or more generically above the critical temperature, the system is in the quantum critical regime.

To be more specific, we consider two vertically coupled quantum dots, the first of which has an attractive reduced BCS coupling, while the second has no BCS coupling. Fig. 1 shows the geometry, the reason for which will become clear soon. We apply an orbital magnetic flux only through (a part of) the second dot, and observe the effect on the coupled system. Our main results are for the mean-field critical temperature T_c of the system, and its magnetization in the normal state (above T_c) as a function of the flux in the normal nanoparticle. Such a system could be realized physically without too much difficulty, by, for example, growing a thin film of normal metal (such as Au) on an insulating substrate, then a layer of insulator which could serve as the hopping bridge, and finally a thin film of superconductor(such as Al, which has a mean-field superconducting transition temperature of around $2.6K$). The orbital flux can be applied selectively to the Au layer as shown in Fig. 1 by a close pair of oppositely oriented current carrying wires close to the Au quantum dot, but far from the Al quantum dot.

The reason for this geometry is that we want to disregard interdot charging effects entirely and concentrate on the BCS coupling. The Hamiltonian for the coupled interacting system contains charging energies for the two dots and an interdot Coulomb interaction[24].

$$\frac{U_1}{2}N_1^2 + \frac{U_2}{2}N_2^2 + U_{12}N_1N_2 \tag{5}$$

Defining the total number of particles as $N = N_1 + N_2$, and the difference in the number as $n = N_1 - N_2$ the interaction can also be written as

$$\frac{U_1 + U_2 + 2U_{12}}{16}N^2 + \frac{U_1 + U_2 - 2U_{12}}{16}n^2 + \frac{U_1 - U_2}{4}nN \tag{6}$$

We see that there is an energy cost to transfer an electron from one dot to the other. This interaction is irrelevant in the RG sense[24], but vanishes only asymptotically deep within an energy scale defined by the hopping. Our geometry is chosen so as to make $U_1 = U_2 = U_{12}$ as nearly as possible, which can be achieved by making the dots the same thickness and area, and by making sure that their vertical separation is much smaller than their lateral linear size. In this case, since N is constant, we can ignore charging effects entirely. Charging effects and charge quantization in finite systems can be taken into account using the formalism developed by Kamenev and Gefen[39], and futher elaborated by Efetov and co-workers[40,41]. Since our primary goal is to investigate quantum critical effects associated with the BCS pairing interaction, we will assume the abovementioned geometry and ignore charging effects in what follows.

After including the effect of the BCS interaction, we find the surprising result that in certain regimes of interparticle hopping strength, the mean-field transition temperature of the system can *increase* as the flux through the second quantum dot increases. Indeed, its behavior can be monotonic increasing, monotonic decreasing, or nonmonotonic as the flux is increased. We can qualitatively understand these effects by the following considerations. In the absence of orbital flux, hopping between the dots reduces T_c since it "dilutes" the effect of the attractive BCS coupling present only in the first dot. The application of an orbital flux through the second dot has two effects: (i) To raise the energy of Cooper pairs there, thus tending to localize the pairs in the first dot and raise the T_c. (ii) To cause time-reversal breaking in the first dot, and reduce T_c. The nonmonotonicity of T_c arises from the competition between these two effects.

Another quantity of interest above the mean-field T_c is the fluctuation magnetization[42], which corresponds to *gapped* superconducting pairs forming and responding to the external orbital flux. In contrast to the case of a single quantum dot subjected to an orbital flux, we find that the fluctuation magnetization[42] can be either diamagnetic (the usual case) or paramagnetic. A paramagnetic magnetization results from a free energy which decreases as the flux increases. The origin of this effect is the interplay between the localizing effect of high temperature or the orbital flux in the second dot on the one hand, and the reduced BCS interaction on the other.

The regimes we describe should be distinguished from other superconducting single-particle RMT ensembles discovered in the past decade[43,44], which apply to a normal meso-

scopic system in contact with two superconductors with a phase difference of π between their order parameters[43] (so that there is no gap in the mesoscopic system despite Andreev reflection), or to a mesoscopic d-wave superconducting system[44]. In our case, the symmetry of the superconducting interaction is s-wave. However, the most important difference is that we focus on quantum critical fluctuations, which are inherently many-body, while the RMT classes described previously are single-particle ensembles[43,44].

This paper is organized as follows. In Sec. II we review the basic steps of calculating the one-particle and two-particle Green's functions for a single dot. Then in Sec. III we present the system of Dyson equations for the one-particle Green's function in the case of two coupled dots and solve it in the limit of weak coupling. In addition, we set up and solve the system of four Bethe-Salpeter equations for the two-particle Green's function. In Sec. IV we apply our results to the system of superconducting quantum dot weakly coupled to other quantum dot made from a normal metal. We end with our conclusions, some caveats, and future directions in Sec. V.

II. REVIEW OF RESULTS FOR A SINGLE DOT.

Our goal in this section is to calculate the statistics of one and two-particle Green's functions for an uncoupled dot in a GOE→ GUE crossover (see appendix A, and[12] for more details), starting from the series expansion of Green's function:

$$\langle\beta|G^R(E)|\alpha\rangle = G^R_{\alpha\beta}(E) = \left(\frac{1}{E^+ - H}\right)_{\alpha\beta} = \frac{\delta_{\alpha\beta}}{E^+} + \frac{H_{\alpha\beta}}{(E^+)^2} + \frac{H^2_{\alpha\beta}}{(E^+)^3} + \ldots. \tag{7}$$

We are interested in averaging this expansion over the appropriate random matrix ensemble. The corresponding Dyson equation for averaged Green's function is:

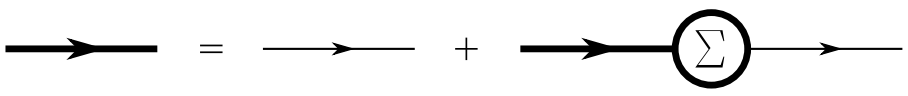

(8)

The bold line denotes the averaged propagator $\langle G^R(E)\rangle$ and regular solid line defines the bare propagator $1/E^+$ with $E^+ = E + i\eta$, where η is infinitely small positive number. Here Σ stands for self-energy and is a sum of all topologically different diagrams.

One can solve Dyson equation approximating self-energy only by first leading term and

find:

$$\Sigma = \frac{E}{2} - \frac{i}{2}\sqrt{\left(\frac{2N\delta}{\pi}\right)^2 - E^2}, \tag{9}$$

where δ is the mean level spacing. This approximation works only for $E \gg \delta$. As E gets comparable with δ, other terms in expansion for Σ should be taken into account.

Then, the average of the one-particle Green's function is given by:

$$\langle G^R_{\alpha\beta}(E)\rangle = \frac{\delta_{\alpha\beta}}{\frac{E}{2} + \frac{i}{2}\sqrt{\left(\frac{2N\delta}{\pi}\right)^2 - E^2}} \tag{10}$$

Next, we repeat the procedure for the averaged two-particle Green's function, which can be represented by the series:

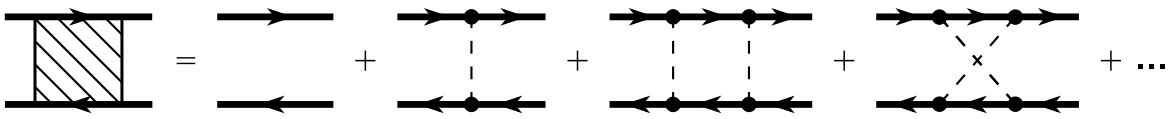

(11)

where two bold lines on the left hand side denote $\langle G^R(E+\omega)G^A(E)\rangle$. The leading contribution comes from ladder and maximally crossed diagrams. The sum of these diagrams can be conveniently represented by Bethe-Salpeter equation. For example, the contribution of all the ladder diagrams can be expressed in closed form by:

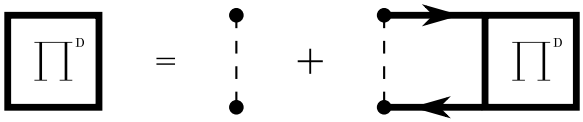

(12)

where Π^D is a self-energy. For maximally crossed diagrams we have similar equation:

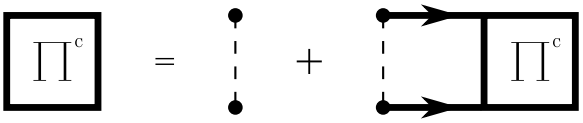

(13)

where Π^D and Π^C are related to the connected part of two-particle Green's function as:

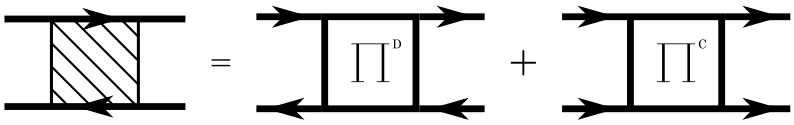

(14)

In the limit of ω being much smaller than bandwidth ($\omega \ll N\delta$), the two-particle Green's function (connected part) is expressed as:

$$\langle G^R_{\alpha\gamma}(E+\omega)G^A_{\delta\beta}(E)\rangle = \frac{2\pi}{N^2\delta}\frac{\delta_{\alpha\beta}\delta_{\gamma\delta}}{-i\omega} + \frac{2\pi}{N^2\delta}\frac{\delta_{\alpha\delta}\delta_{\gamma\beta}}{-i\omega}\frac{1}{1+i\frac{E_X}{\omega}} \tag{15}$$

The second term is a contribution of maximally crossed diagrams. E_X is a crossover energy scale, connected to the crossover parameter as $E_X = 4X^2 N\delta/\pi$.

Depending on values of E_X one can speak of different types of averaging. If $E_X \ll \omega$, we get average over GOE ensemble, if E_X is of order ω, averaging is performed over ensemble being in crossover, and, if $E_X \gg \omega$, contribution of maximally crossed diagrams can be disregarded, thus going to the limit of the GUE ensemble.

III. TWO COUPLED DOTS.

Next we discuss general framework of our calculation and calculate correlation functions for our system of interest, which is two weakly coupled quantum dots (see appendix B for more technical details). The Hamiltonian for this system can be represented as:

$$H_{tot} = \begin{pmatrix} H_1 & 0 \\ 0 & H_2 \end{pmatrix} + \begin{pmatrix} 0 & V \\ V^\dagger & 0 \end{pmatrix} = \begin{pmatrix} H_1 & V \\ V^\dagger & H_2 \end{pmatrix}. \tag{16}$$

where H_1 and H_2 are the Hamiltonians of uncoupled dots 1 and 2. The coupling is realized by a matrix V. The elements of H_1, H_2, and V are statistically independent random variables. We assume that both dots and the hopping bridge are in crossover regimes, characterized by parameters X_1, X_2, and Γ respectively.

In the crossover matrices H_i and V are given by:

$$H_i = \frac{H_i^S + iX_i H_i^A}{\sqrt{1+X_i^2}},\ i = 1,2; \qquad V = \frac{V^R + i\Gamma V^I}{\sqrt{1+\Gamma^2}}, \tag{17}$$

where $H_i^{S,A}$ is a symmetric (antisymmetric) part of H_i, and $V^{R,I}$ is real (imaginary) matrix. In what follows we assume that the bandwidths in dot 1 and dot 2 are the same. That is, $N_1\delta_1 = N_2\delta_2$. This should not make any difference in the universal limit $N \to \infty$. In addition we introduce the parameter ξ – the ratio of mean level spacing in two dots: $\xi = \delta_1/\delta_2$. For each realization of matrix elements of the Hamiltonian H_{tot}, the Green's function of this system can be computed as follows:

$$G = (I \otimes E - H)^{-1} = \begin{pmatrix} E - H_1 & -V \\ -V^\dagger & E - H_2 \end{pmatrix}^{-1} = \begin{pmatrix} G_{11} & G_{12} \\ G_{21} & G_{22} \end{pmatrix}. \tag{18}$$

Each element of G has the meaning of a specific Green's function. For example, G_{11} and G_{22} are the Green's functions that describe particle propagation in dots 1 and 2 respectively.

On the other hand, G_{12} and G_{21} are the Green's functions representing travel from one dot to another.

Calculating $(I \otimes E - H)^{-1}$ one finds the components of G. For example,

$$G_{11} = \left[(E - H_1) - V(E - H_2)^{-1}V^\dagger\right]^{-1} = G_1 + G_1VG_2V^\dagger G_1 + G_1VG_2V^\dagger G_1VG_2V^\dagger G_1 + \dots \tag{19}$$

where G_1 and G_2 are bare propagators in dot 1 and dot 2 defined by $G_1 = (E - H_1)^{-1}$ and $G_2 = (E - H_2)^{-1}$.

To find the ensemble average of G_{11} one needs to average the whole expansion (19) term by term. For coupled dots G_{ij} interrelated and in large N approximation can be found from the following system of equations:

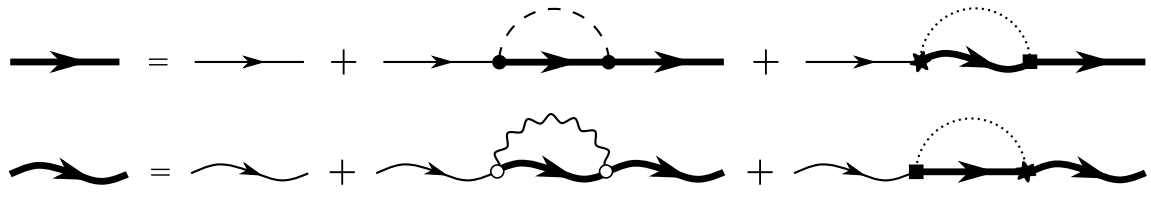

(20)

The bold straight and wavy lines with arrows represent averaged Green's functions $\langle G_{\alpha\beta,1}(E)\rangle$ and $\langle G_{ij,2}(E)\rangle$ respectively, while regular solid lines are bare propagators in dots 1 and 2. The dotted line describes pairing between hopping matrix elements V, and the dashed (wavy) line denotes pairing between matrix elements of H_1 (H_2).

The system (20) accounts for all possible diagrams without line crossing. Diagrams containing crossed lines of any type are higher order in $1/N$ and can be neglected when $N \to \infty$. If the hopping between dots is zero, this system decouples into two separate Dyson equations for each dot. In the case of weak coupling ($U \ll 1$), where U is a parameter controlling the strength of coupling between dots, this system can be readily solved. As zero approximation, we use results for a single dot.

In this approximation one-particle Green's function for dot 1 and dot 2 are calculated as follows:

$$\langle G^R_{\alpha\beta,1}(E)\rangle = \frac{\langle G^R_{\alpha\beta,0}(E)\rangle}{1-U\sqrt{\xi}\frac{\Sigma_0}{E-2\Sigma_0}} = \frac{\delta_{\alpha\beta}}{\left(\frac{N_1\delta_1}{\pi}\right)\left[\epsilon+i\sqrt{1-\epsilon^2}\right]}\frac{1}{\left[1+\frac{U\sqrt{\xi}}{2}\left(1+i\frac{\epsilon}{\sqrt{1-\epsilon^2}}\right)\right]}$$
$$\langle G^R_{ij,2}(E)\rangle = \frac{\langle G^R_{ij,0}(E)\rangle}{1-\frac{U}{\sqrt{\xi}}\frac{\Sigma_0}{E-2\Sigma_0}} = \frac{\delta_{ij}}{\left(\frac{N_2\delta_2}{\pi}\right)\left[\epsilon+i\sqrt{1-\epsilon^2}\right]}\frac{1}{\left[1+\frac{U}{2\sqrt{\xi}}\left(1+i\frac{\epsilon}{\sqrt{1-\epsilon^2}}\right)\right]}, \tag{21}$$

where ϵ is a dimensionless energy $\epsilon = \pi E/2N\delta$. We used subindex 0 in Σ_0 and $\langle G^R_0(E)\rangle$ to denote solutions for one uncoupled dot.

In the large N approximation the contribution to the two-particle Green's function comes from ladder diagrams and maximally crossed diagrams. It is convenient to sum them separately. The ladder diagram contribution can be found from the following system of equations:

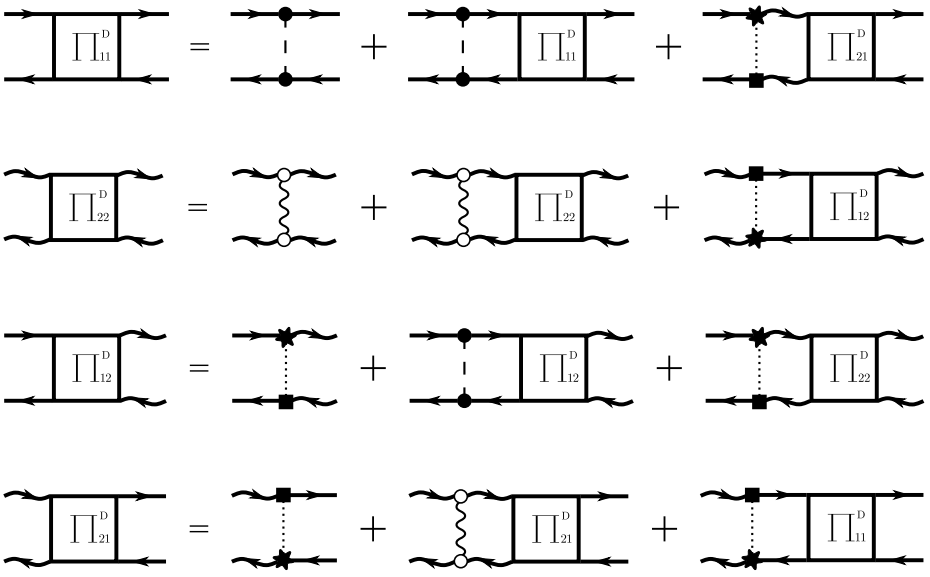

(22)

where Π^D_{ij} with proper external lines denote various two-particle Green's functions. As in the case of the one-particle Green's function equations, if the inter-dot coupling is zero, the system reduces to two Bethe-Salpeter equations for uncoupled dots.

The system of four equations (22) can be broken into two systems of two equations to get:

$$\langle G^R_{\alpha\gamma,1}(E+\omega)G^A_{\delta\beta,1}(E)\rangle_{D1} = \frac{2\pi}{N_1^2\delta_1}\frac{\delta_{\alpha\beta}\delta_{\gamma\delta}}{-i\omega}g_{D1}$$
$$\langle G^R_{il,2}(E+\omega)G^A_{kj,2}(E)\rangle_{D2} = \frac{2\pi}{N_2^2\delta_2}\frac{\delta_{ij}\delta_{lk}}{-i\omega}g_{D2},$$

where g_D are the scaling functions of diffusion terms in dot 1 and dot 2 defined by:

$$\begin{aligned} g_{D1} &= \frac{1+\frac{i}{\sqrt{\xi}}\frac{E_U}{\omega}}{1+i(\sqrt{\xi}+\frac{1}{\sqrt{\xi}})\frac{E_U}{\omega}} \\ g_{D2} &= \frac{1+i\sqrt{\xi}\frac{E_U}{\omega}}{1+i(\sqrt{\xi}+\frac{1}{\sqrt{\xi}})\frac{E_U}{\omega}}. \end{aligned} \tag{23}$$

Here $E_U = 2UN\delta/\pi$ is the interdot coupling energy scale. These dimensionless functions show how diffusion part is modified due to the coupling to another dot.

Next, for the maximally crossed diagrams the system of equations we have:

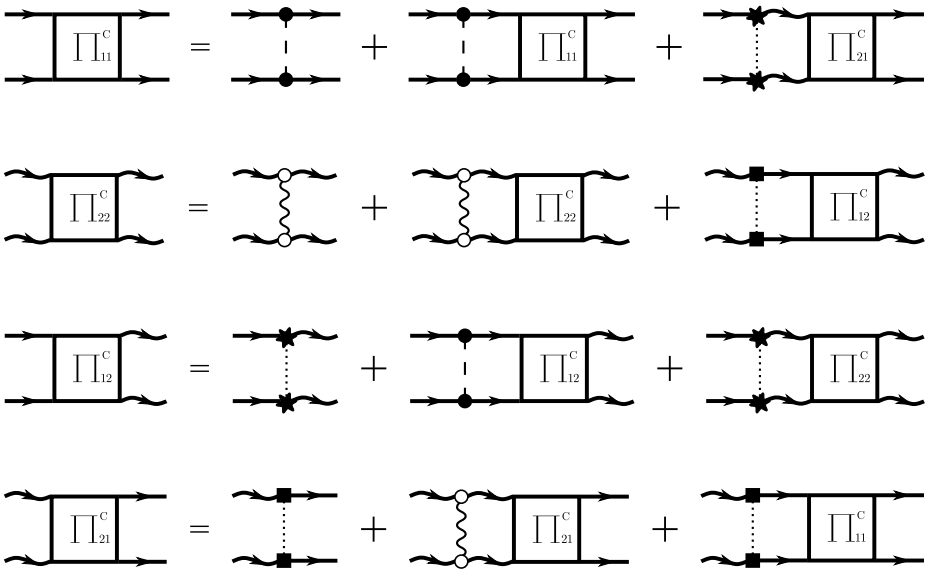

(24)

The subsequent solution of this system produces:

$$\begin{aligned} \langle G^R_{\alpha\gamma,1}(E+\omega)G^A_{\delta\beta,1}(E)\rangle_{C1} &= \frac{2\pi}{N_1^2\delta_1}\frac{\delta_{\alpha\delta}\delta_{\gamma\beta}}{-i\omega}g_{C1} \\ \langle G^R_{il,2}(E+\omega)G^A_{kj,2}(E)\rangle_{C2} &= \frac{2\pi}{N_2^2\delta_2}\frac{\delta_{ik}\delta_{lj}}{-i\omega}g_{C2}, \end{aligned} \tag{25}$$

where g_C are the scaling functions for cooperon term defined according to:

$$\begin{aligned} g_{C1} &= \frac{1+\frac{i}{\sqrt{\xi}}\frac{E_U}{\omega}+i\frac{E_{X_2}}{\omega}}{1+i\frac{E_{X_1}+E_{X_2}}{\omega}-\frac{E_{X_1}E_{X_2}}{\omega^2}-\frac{E_{X_1}E_U}{\sqrt{\xi}\omega^2}-\frac{\sqrt{\xi}E_{X_2}E_U}{\omega^2}+i\left(\sqrt{\xi}+\frac{1}{\sqrt{\xi}}\right)\frac{E_U}{\omega}\left(1+i\frac{E_\Gamma}{\omega}\right)} \\ g_{C2} &= \frac{1+i\sqrt{\xi}\frac{E_U}{\omega}+i\frac{E_{X_1}}{\omega}}{1+i\frac{E_{X_1}+E_{X_2}}{\omega}-\frac{E_{X_1}E_{X_2}}{\omega^2}-\frac{E_{X_1}E_U}{\sqrt{\xi}\omega^2}-\frac{\sqrt{\xi}E_{X_2}E_U}{\omega^2}+i\left(\sqrt{\xi}+\frac{1}{\sqrt{\xi}}\right)\frac{E_U}{\omega}\left(1+i\frac{E_\Gamma}{\omega}\right)}. \end{aligned} \tag{26}$$

Here $E_{X_{1,2}} = 4X_{1,2}^2 N\delta/\pi$, and $E_\Gamma = 4\Gamma^2 E_U/(\sqrt{\xi} + \frac{1}{\sqrt{\xi}})$ are the crossover energy scales, describing transition from GOE to GUE ensemble in dot 1 and dot 2, as well as in hopping bridge V.

As we determined how the scaling function g_C modifies cooperon part of two-particle Green's function and depends on the crossover energy scales defined above, we are ready to proceed with write up the connected part of the total two-particle Green's function, which is a sum of diffuson and cooperon parts:

$$\langle G^R_{\alpha\gamma,1}(E+\omega)G^A_{\delta\beta,1}(E)\rangle = \frac{2\pi}{N_1^2\delta_1}\frac{\delta_{\alpha\beta}\delta_{\gamma\delta}}{-i\omega}\frac{1+\frac{i}{\sqrt{\xi}}\frac{E_U}{\omega}}{1+i(\sqrt{\xi}+\frac{1}{\sqrt{\xi}})\frac{E_U}{\omega}} + \frac{2\pi}{N_1^2\delta_1}\frac{\delta_{\alpha\delta}\delta_{\gamma\beta}}{-i\omega}\frac{1+\frac{i}{\sqrt{\xi}}\frac{E_U}{\omega}+i\frac{E_{X_2}}{\omega}}{1+i\frac{E_{X_1}+E_{X_2}}{\omega}-\frac{E_{X_1}E_{X_2}}{\omega^2}-\frac{E_{X_1}E_U}{\sqrt{\xi}\omega^2}-\frac{\sqrt{\xi}E_{X_2}E_U}{\omega^2}+i\left(\sqrt{\xi}+\frac{1}{\sqrt{\xi}}\right)\frac{E_U}{\omega}\left(1+i\frac{E_\Gamma}{\omega}\right)} \tag{27}$$

$$\langle G^R_{il,2}(E+\omega)G^A_{kj,2}(E)\rangle = \frac{2\pi}{N_2^2\delta_2}\frac{\delta_{ij}\delta_{lk}}{-i\omega}\frac{1+i\sqrt{\xi}\frac{E_U}{\omega}}{1+i(\sqrt{\xi}+\frac{1}{\sqrt{\xi}})\frac{E_U}{\omega}} + \frac{2\pi}{N_2^2\delta_2}\frac{\delta_{ik}\delta_{lj}}{-i\omega}\frac{1+i\sqrt{\xi}\frac{E_U}{\omega}+i\frac{E_{X_1}}{\omega}}{1+i\frac{E_{X_1}+E_{X_2}}{\omega}-\frac{E_{X_1}E_{X_2}}{\omega^2}-\frac{E_{X_1}E_U}{\sqrt{\xi}\omega^2}-\frac{\sqrt{\xi}E_{X_2}E_U}{\omega^2}+i\left(\sqrt{\xi}+\frac{1}{\sqrt{\xi}}\right)\frac{E_U}{\omega}\left(1+i\frac{E_\Gamma}{\omega}\right)} \tag{28}$$

In general, the coupling between dots changes the bandwidth of each dot. Corrections to the bandwidth are of the order of U and can be neglected for weak coupling. Calculating approximations to the second order in U one can be ensure that one-particle and two-particle Green's functions can be treated perturbatively.

Diagrams on Fig.2 show the typical behavior of absolute value and phase of scaling functions g_D and g_C in dot 1. All energy parameters are measured in units of E_U.

Next we analyze the temporal behavior of the computed statistical characteristics. The Fourier transform of the two-particle Green's function shows the time evolution of the density matrix of the system. One can observe that the diffuson part of $\langle G^R G^A\rangle$ diverges for small ω. To get the correct behavior we replace $1/\omega$ with $\omega/(\omega^2+\eta^2)$, and take η to zero in the final result. As for the cooperon term, it stays regular in the small ω limit if at least one of the crossover parameters differs from zero.

First of all, we look at the Fourier transform of $\langle G^R G^A\rangle$ in the first dot. We have

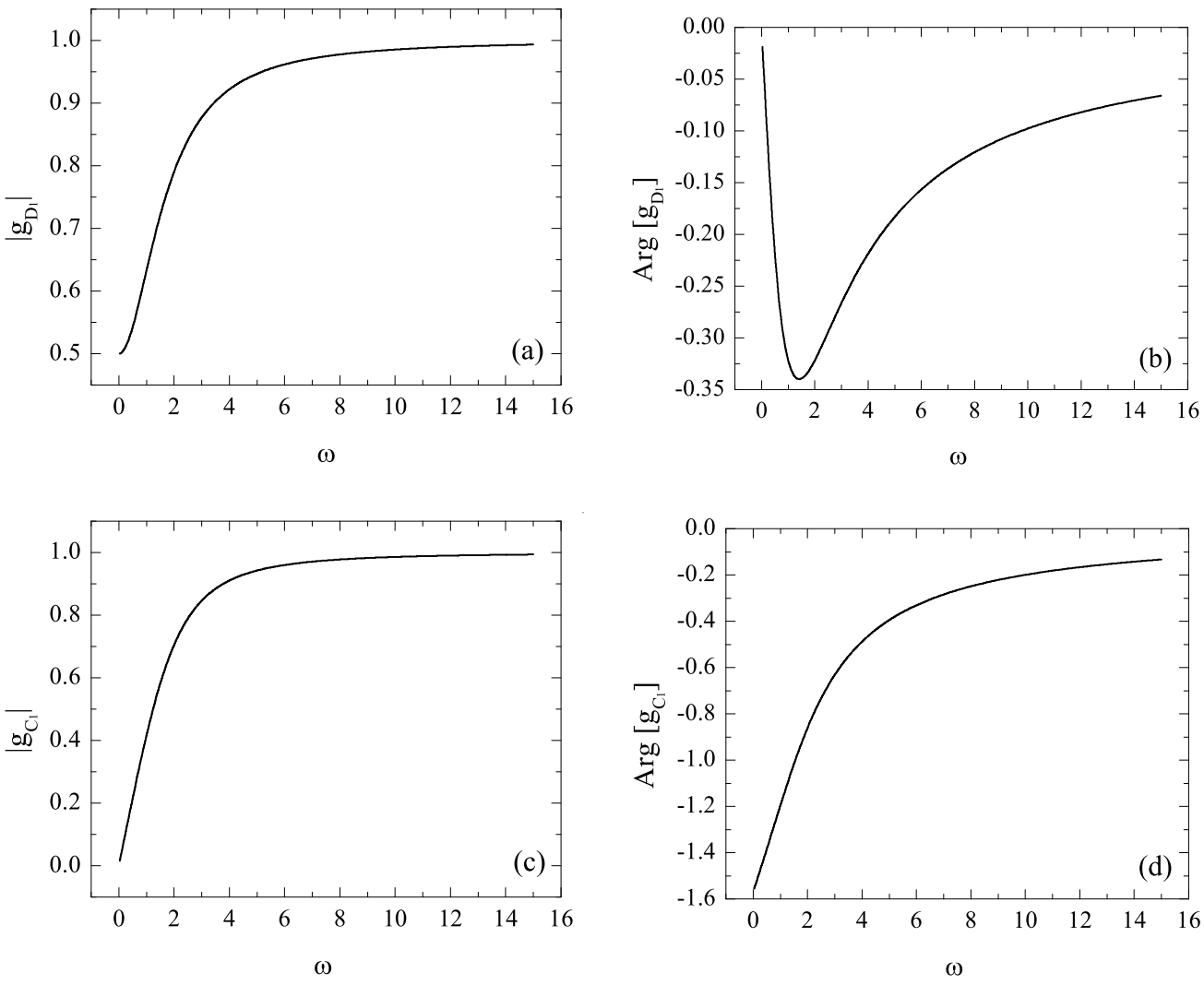

FIG. 2: Absolute value and phase of diffuson (a,b) and cooperon (c,d) scaling functions in dot 1. Frequency ω is measured in units of E_U. For these graphs the crossover parameters are: $E_{X_1}/E_U = E_{X_2}/E_U = 1$, $E_\Gamma/E_U = 0.8$, $\xi = 1$.

$$\langle G^R_{\alpha\gamma,1}(t) G^A_{\delta\beta,1}(t)\rangle = \delta_{\alpha\beta}\delta_{\gamma\delta}\frac{2}{N_1(1+\xi)}\left[\frac{1}{2} + \xi e^{-(\sqrt{\xi}+\frac{1}{\sqrt{\xi}})E_U t}\right] + \delta_{\alpha\delta}\delta_{\gamma\beta}\frac{2}{N_1}\left[1 + \frac{E_{X_2} + \frac{E_U}{\sqrt{\xi}}}{a_+ - a_-}\left(e^{-ta_-} - e^{-ta_+}\right)\right], \quad (29)$$

where $a_\pm$ depend on the crossover parameters (see Eq. (C11) in appendix C)

Then, for the corresponding quantity in the second dot the Fourier transform produces:

$$\langle G^R_{il,2}(t)G^A_{kj,2}(t)\rangle = \delta_{ij}\delta_{lk}\frac{2\xi}{N_2(1+\xi)}\left[\frac{1}{2}+\frac{1}{\xi}e^{-(\sqrt{\xi}+\frac{1}{\sqrt{\xi}})E_U t}\right] + \delta_{ik}\delta_{lj}\frac{2}{N_2}\left[1+\frac{E_{X_1}+\sqrt{\xi}E_U}{a_+-a_-}\left(e^{-ta_-}-e^{-ta_+}\right)\right]. \quad (30)$$

IV. TWO COUPLED METALLIC QUANTUM DOTS

In this section we apply the results obtained in the previous sections to an interacting system. We consider two vertically coupled metallic quantum dots, as shown in Fig. 1, the first of which is superconducting and the second noninteracting. For simplicity the quantum dots are assumed to have the same level spacing ($\xi = 1$). The calculations presented in this section can be extended to the case $\xi \neq 1$ in a straightforward way. The first (superconducting) quantum dot and the hopping bridge belong to the GOE ensemble. A nonzero orbital magnetic flux penetrating the second (noninteracting) quantum dot drives it into the GOE to GUE crossover described by the crossover energy scale E_{X_2}. The other crossover energy scale E_U describes the hopping between the quantum dots. Because of this hopping one can observe a nonzero magnetization in the first particle caused by a magnetic flux through the second particle. Roughly speaking, when the electrons in the first dot travel to the second and return they bring back information about the orbital flux.

We wish to compute the magnetization as a function of orbital flux, as well as the mean-field critical temperature. It should be noted that since the quantum dot is a finite system, there cannot be any true spontaneous symmetry breaking. However, when the mean-field superconducting gap $\Delta_{BCS} \gg \delta$, the mean-field description is a very good one[45,46,47]. Recent numerical calculations have investigated the regime $\Delta_{BCS} \simeq \delta$ where quantum fluctuations are strong[48]. We will focus on the quantum critical regime of the system above the mean-field critical temperature/field, so we do not have to worry about symmetry-breaking.

We start with BCS crossover Hamiltonian for the double-dot system including the interactions in the first dot and the hopping between the dots[26]:

$$H_{BCSX_2} = \sum_{\mu_0\nu_0} H^{(1)}_{\mu_0\nu_0} c^\dagger_{\mu_0 s} c_{\nu_0 s} - \lambda T^\dagger T + \sum_{i_0 j_0 s} H^{(2)}_{i_0 j_0 s} c^\dagger_{i_0 s} c_{i_0 s} + \sum_{\mu_0 i_0} V_{\mu_0 i_0} (c^\dagger_{\mu_0 s} c_{i_0 s} + h.c.)$$
$$= \sum_{\mu s} \epsilon_\mu c^\dagger_{\mu,s} c_{\mu,s} - \delta\tilde{\lambda} T^\dagger T, \tag{31}$$

where $H^{(2)}$ contains the effect of the orbital flux through the second quantum dot. Here T, $T^\dagger$ are the operators which appear in the Universal Hamiltonian, and are most simply expressed in terms of electron creation/annihilation operators in the original GOE basis of the first dot (which we call μ_0, ν_0) as

$$T = \sum_{\mu_0} c_{\mu_0,\downarrow} c_{\mu_0,\uparrow} \tag{32}$$

Now we need to express the operators $c_{\mu_0,s}$ in terms of the eigenoperators of the combined single-particle Hamiltonian of the system of two coupled dots. The result is

$$T = \sum_{\mu\nu} M_{\mu\nu} c_{\nu,\downarrow} c_{\mu,\uparrow}, \qquad M_{\mu\nu} = \sum_{\mu_0} \psi_\mu(\mu_0)\psi_\nu(\mu_0), \tag{33}$$

where ϵ_μ denotes the eigenvalues of the total system, $c_{\mu,s}$ operator annihilates electron in the orbital state μ with spin s, $\psi_\mu(\mu_0)$ is the eigenvector of the compound system, δ is the mean level spacing of a single isolated dot, $\tilde{\lambda} > 0$ is the attractive dimensionless BCS coupling valid in region of width $2\omega_D$ around the Fermi energy. Note that while the indices μ, ν enumerate the states of the total system, the index μ_0 goes only over the states of the first dot, since the superconducting interaction is present only in the first dot.

To study the magnetization of the first quantum dot in the crossover we follow previous work by one of us[26]: We start with the partition function $Z = Tr(exp{-}\beta H)$ where $\beta = 1/T$ is the inverse temperature. We convert the partition function into an imaginary time path integral and use the Hubbard-Stratanovich identity to decompose the interaction, leading to the imaginary time Lagrangian

$$\mathcal{L} = \frac{|\sigma|^2}{\delta\tilde{\lambda}} - \sum_{\mu,s} \bar{c}_{\mu,s}(\partial_\tau - \epsilon_\mu) c_{\mu,s} + \sigma\bar{T} + \bar{\sigma}T \tag{34}$$

where $\sigma, \bar{\sigma}$ are the bosonic Hubbard-Stratanovich fields representing the BCS order parameter and $\bar{c}, c$ are Grassman fields representing fermions. The fermions are integrated out, and

as long as the system does not have a mean-field BCS gap, the resulting action for $\sigma, \bar{\sigma}$ can be expanded to second order to obtain

$$S_{eff} \approx \frac{\delta}{\beta} \sum_n \ |\sigma(i\omega_n)|^2 (\tfrac{1}{\tilde{\lambda}} - f_n(\beta, E_X, \omega_D)) \tag{35}$$

$$f_n(\beta, E_X, \omega_D) = \quad \delta \sum_{\mu\nu} |M_{\mu\nu}|^2 \tfrac{1-N_F(\epsilon_\mu)-N_F(\epsilon_\nu)}{\epsilon_\mu+\epsilon_\nu-i\omega_n} \tag{36}$$

where $\omega_n = 2\pi n/\beta$, and the sums are restricted to $|\epsilon_\mu|, |\epsilon_\nu| < \hbar\omega_D$. We see that the correlations between different states μ, ν play an important role. Deep in the crossover (for $E_X \gg \delta$) we can replace $|M_{\mu\nu}|^2$ by its ensemble average[26]. We will also henceforth replace the summations over energy eigenstates by energy integrations with the appropriate cutoffs. In previous work[26] the statistics[23,24,25] of $|M_{\mu\nu}|^2$ was used to obtain analytical results for this expression.

The (interacting part of the) free energy of the system in the quantum critical regime is given by[26]:

$$\beta F = \sum_n \ln(1 - \tilde{\lambda} f(i\omega_n, \beta, E_{X_2})), \tag{37}$$

where f is the scaling function given by expression:

$$f(i\omega_n, \beta, E_{X_2}) = \delta \sum_{\mu\nu} |M_{\mu\nu}|^2 \frac{1 - n_\mu(\beta) - n_\nu(\beta)}{\epsilon_\mu + \epsilon_\nu - i\omega_n}, \tag{38}$$

$n_\nu(\beta) = (1 + \exp(\beta\epsilon_\nu))^{-1}$ is the Fermi-Dirac distribution. We have shifted the energy so that the chemical potential is 0.

Converting this double sum into integral and substituting $|M_{\mu\nu}|^2$ by its ensemble average (see Appendices D and E), we get:

$$f_n = \frac{E_U}{\pi} \int_{-\omega_D}^{\omega_D} d\epsilon_1 d\epsilon_2 \frac{(\epsilon_1 - \epsilon_2)^2 + E_{X_2} E_U + E_{X_2}^2}{((\epsilon_1 - \epsilon_2)^2 - E_{X_2} E_U)^2 + (E_{X_2} + 2E_U)^2 (\epsilon_1 - \epsilon_2)^2} \frac{\tanh(\frac{\beta\epsilon_1}{2}) + \tanh(\frac{\beta\epsilon_2}{2})}{\epsilon_1 + \epsilon_2 - i\omega_n}, \tag{39}$$

where ω_D is the Debye frequency, and $\beta = 1/k_B T$ is the inverse temperature.

One can decompose the ratio in the first part of integrand into two Lorentzians to get[26]:

$$f_n = \frac{E_U}{2E_1}\frac{E_{X_2}^2 + E_U E_{X_2} - E_1^2}{E_2^2 - E_1^2}\ln\left[\frac{4(\hbar\omega_D)^2 + \omega_n^2}{C'/\beta^2 + (E_1 + |\omega_n|)^2}\right] + \frac{E_U}{2E_2}\frac{E_2^2 - E_{X_2}^2 - E_U E_{X_2}}{E_2^2 - E_1^2}\ln\left[\frac{4(\hbar\omega_D)^2 + \omega_n^2}{C'/\beta^2 + (E_2 + |\omega_n|)^2}\right]. \quad (40)$$

Here $C' \approx 3.08$ and $E_{1,2}$ depend on crossover energy scales as follows:

$$E_{1,2}^2 = \frac{1}{2}\left[(E_{X_2} + 2E_U)^2 - 2E_U E_{X_2} \mp \sqrt{(E_{X_2} + 2E_U)^2(E_{X_2}^2 + 4E_U^2)}\right]. \quad (41)$$

The magnetization can then be obtained from the free energy:

$$M = -\frac{\partial F}{\partial B} = M_{nonint} + \frac{\tilde{\lambda}L^2}{\beta}\frac{\partial E_{X_2}}{\partial \phi}\sum_n \frac{\frac{\partial f_n}{\partial E_{X_2}}}{1 - \tilde{\lambda} f_n}, \quad (42)$$

where M_{nonint} is the contribution from noninteracting electrons[49]. We will be interested in the second term, which is the fluctuation magnetization[42].

For illustrative purposes, we use the parameters for Al in all our numerical calculations, with $\omega_D = 34meV$ and $\tilde{\lambda} = 0.193$. This leads to a mean-field transition temperature $T_{c0} = 0.218meV = 2.6K$ for an isolated Al quantum dot in the absence of magnetic flux. In all our calculations we evaluate Matsubara sums with a cutoff $\exp -|\omega_n|/\omega_D$. We have verified that changing the cutoff does not qualitatively affect our results, but only produces small numerical changes.

It will be informative to compare the two-dot system with a single dot subject to an orbital magnetic flux[26] (see Fig. 3). We draw the reader's attention to two important features. Firstly, the critical temperature T_c decreases monotonically with E_X, resulting from the fact that time-reversal breaking disfavors superconductivity. Secondly, the fluctuation magnetization is always negative, or diamagnetic, resulting from the fact that the free energy monotonically increases as the orbital flux increases.

Now let us turn to our system of two quantum dots coupled by hopping. Before we carry out a detailed analysis, it is illuminating to inspect the behavior of $E_{1,2}$ and the coefficients of the two logarithms in Eq. (40) (which we call $A_{1,2}$) as a function of E_{X_2}. This is shown in Fig. 4. E_1 tends to $E_{X_2}/2$ for $E_{X_2} \ll E_U$, and to E_U in the opposite limit $E_{X_2} \gg E_U$. E_2 tends to E_U for $E_{X_2} \ll E_U$, while in the opposite limit $E_{X_2} \gg E_U$ $E_2 \to E_{X_2}$. Both coefficients $A_{1,2}$ start at $\frac{1}{2}$ for small E_{X_2}. For $E_{X_2} \gg E_U$ $A_1 \to 1$, while $A_2 \to 0$.

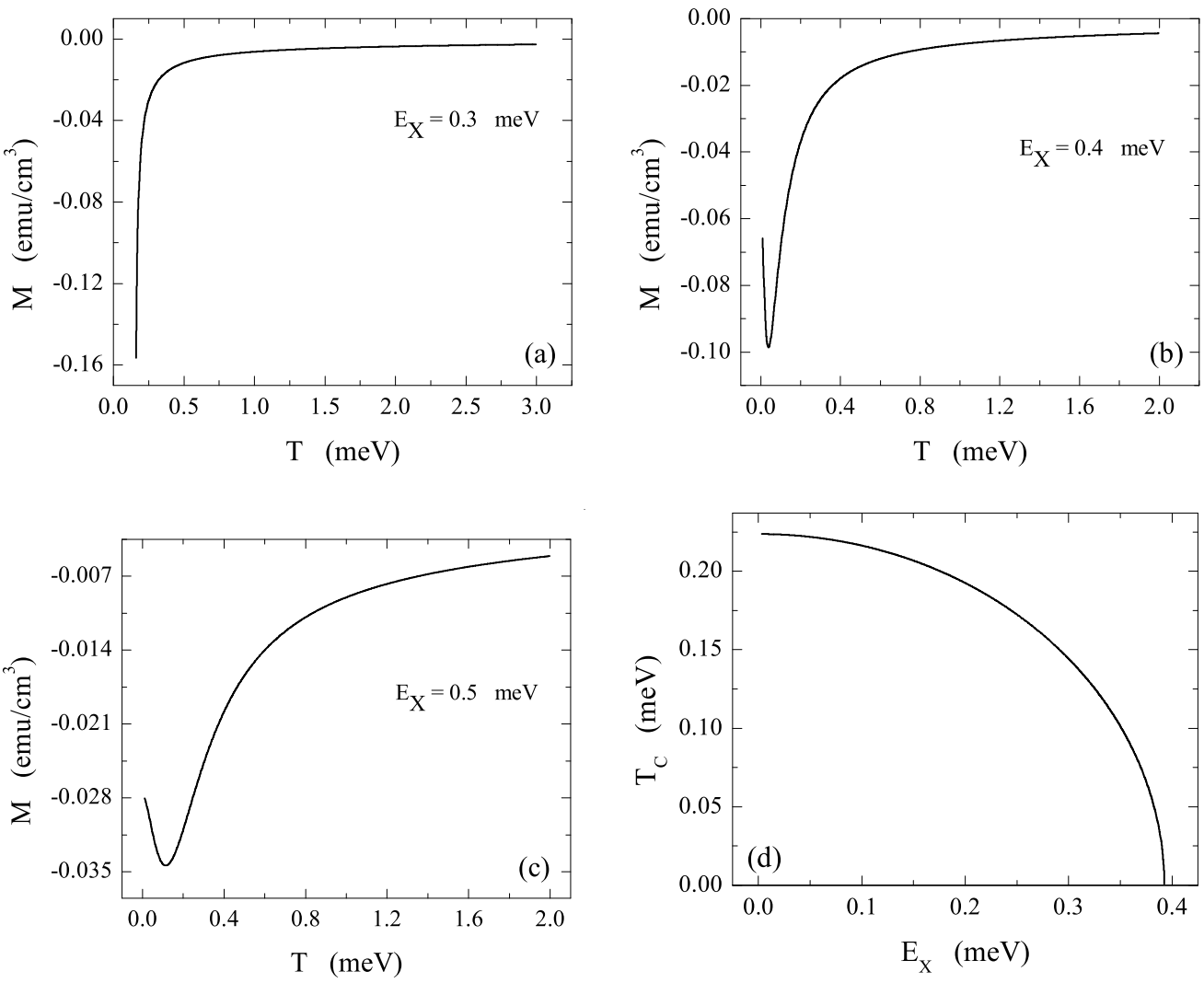

FIG. 3: Magnetization (per unit volume) in a single dot system as a function of temperature for different values of crossover parameters E_X. Panel (d) shows the dependence of the critical temperature on E_X.

The asymptotic regimes $T, E_{X_2} \ll E_U$ and $T, E_{X_2} \gg E_U$ can be understood simply. In the first regime, E_U is the largest energy scale, and far below it the spatial information that there are two distinct quantum dots is lost. The system behaves like a single large dot with a smaller "diluted" superconducting coupling. On the other hand, when $T, E_{X_2} \gg E_U$, A_2 is vanishingly small, and the system resembles the isolated first dot with a superconducting coupling $\tilde{\lambda}$ but with a crossover energy E_U. Note that the approach of the energies to the asymptotes is slow, so for a particular value of E_U it may happen that one cannot realistically

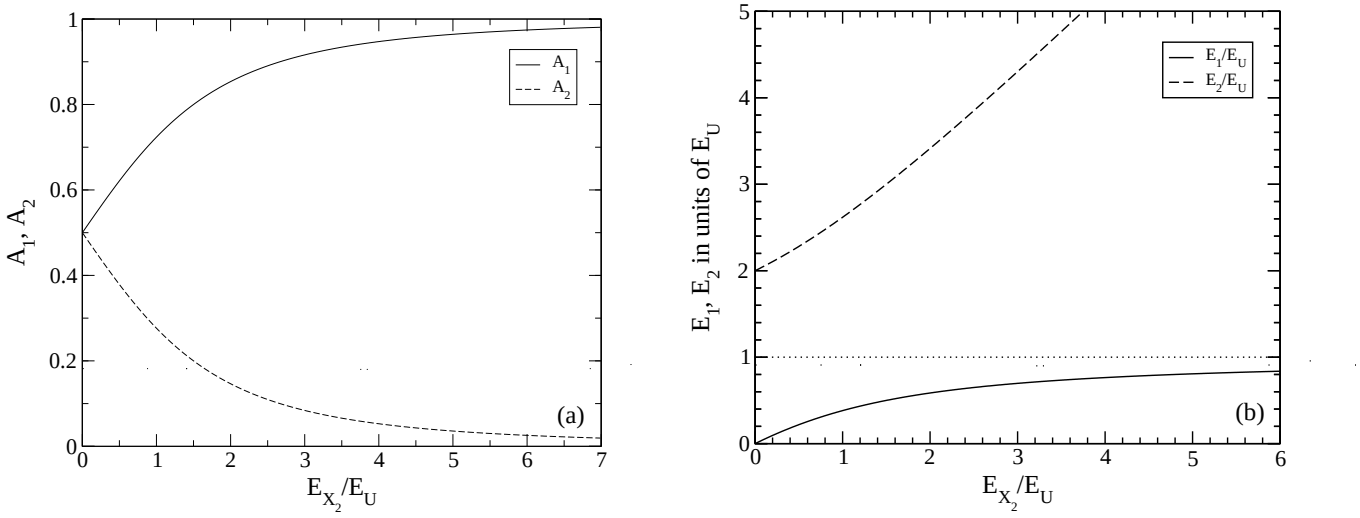

FIG. 4: The behavior of Log coefficients in Eq. (40) and E_1,E_2 as functions of the ratio E_{X_2}/E_U.

approach the asymptotic regime without running into either δ at the lower end or ω_D at the higher end. Finally, one can envisage situations in which $E_{X_2} \ll E_U$ but $T \geq E_U$, for which there are no simple pictures.

The temperature dependence of magnetization per unit volume for different values of crossover parameters E_{X_2} and E_U (excluding the part due to noninteracting electrons) is shown in Fig. 5.

In the range where magnetization changes significantly, the fluctuation magnetization shows both diamagnetic and paramagnetic behavior. This is in contrast to the case of a single superconducting quantum dot subjected to an orbital flux where the fluctuation magnetization is always diamagnetic (Fig. 3). Close to $T = 0$ an increase in temperature makes the fluctuation magnetization more diamagnetic. A further temperature increase changes the fluctuation magnetization from diamagnetic to paramagnetic. For large values of temperature the fluctuation magnetization is paramagnetic and decreasing as T increases. Another set of diagrams, Fig. 6, demonstrates the dependence of the fluctuation magnetization in the first dot on crossover parameter E_{X_2} in the second dot. Generically, we find that at low T the fluctuation magnetization is diamagnetic while at high T it is paramagnetic.

The variation of crossover energy scales E_{X_2} and E_U does not change the qualitative behavior of the fluctuation magnetization as a function of T or E_{X_2}. A paramagnetic magnetization is counterintuitive in superconducting system, because one believes that "an orbital flux is the enemy of superconductivity", and therefore that the free energy must

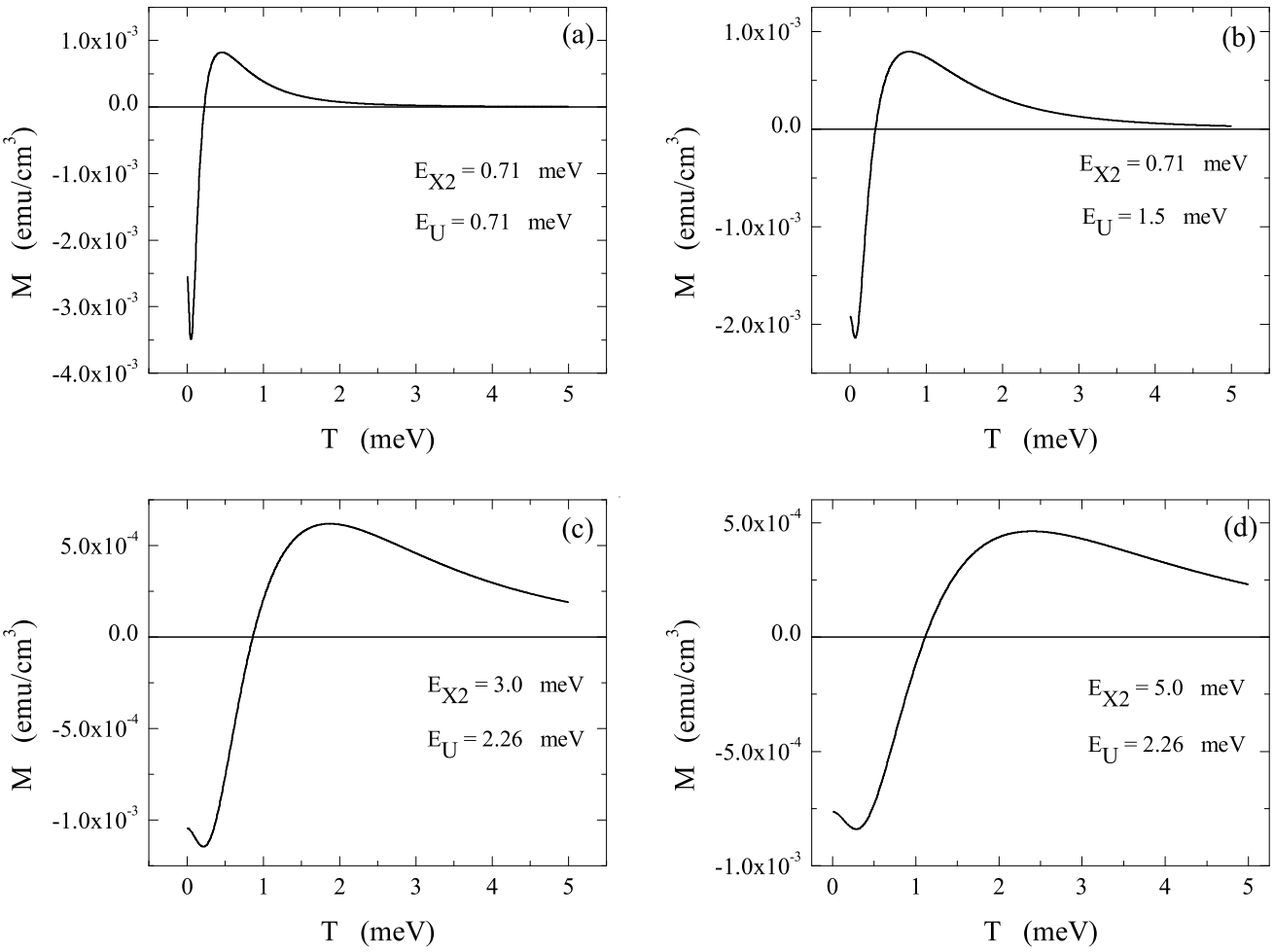

FIG. 5: Magnetization (per unit volume) as a function of temperature for different values of crossover parameters E_{X_2} and E_U. The fluctuation magnetization is diamagnetic for low T and paramagnetic for high T.

always increase as the orbital flux increases. This assumption is false for our system. The explanation is fairly simple, as we will see immediately after the results for T_c have been presented.

The mean-field critical temperature T_c of transition between normal and superconducting state strongly depends on E_{X_2} and E_U. As one can see from Fig. 7, for very strong hopping ($E_U \gg T_{c0}$) between quantum dots T_c is monotonically decreasing as E_{X_2} increases. On the other hand, for intermediate hopping T_c has a maximum as a function of orbital flux, which means that for small values of orbital magnetic flux T_c *increases as the orbital flux increases*. Finally, when E_U is very weak, T_c *monotonically increases* as a function of

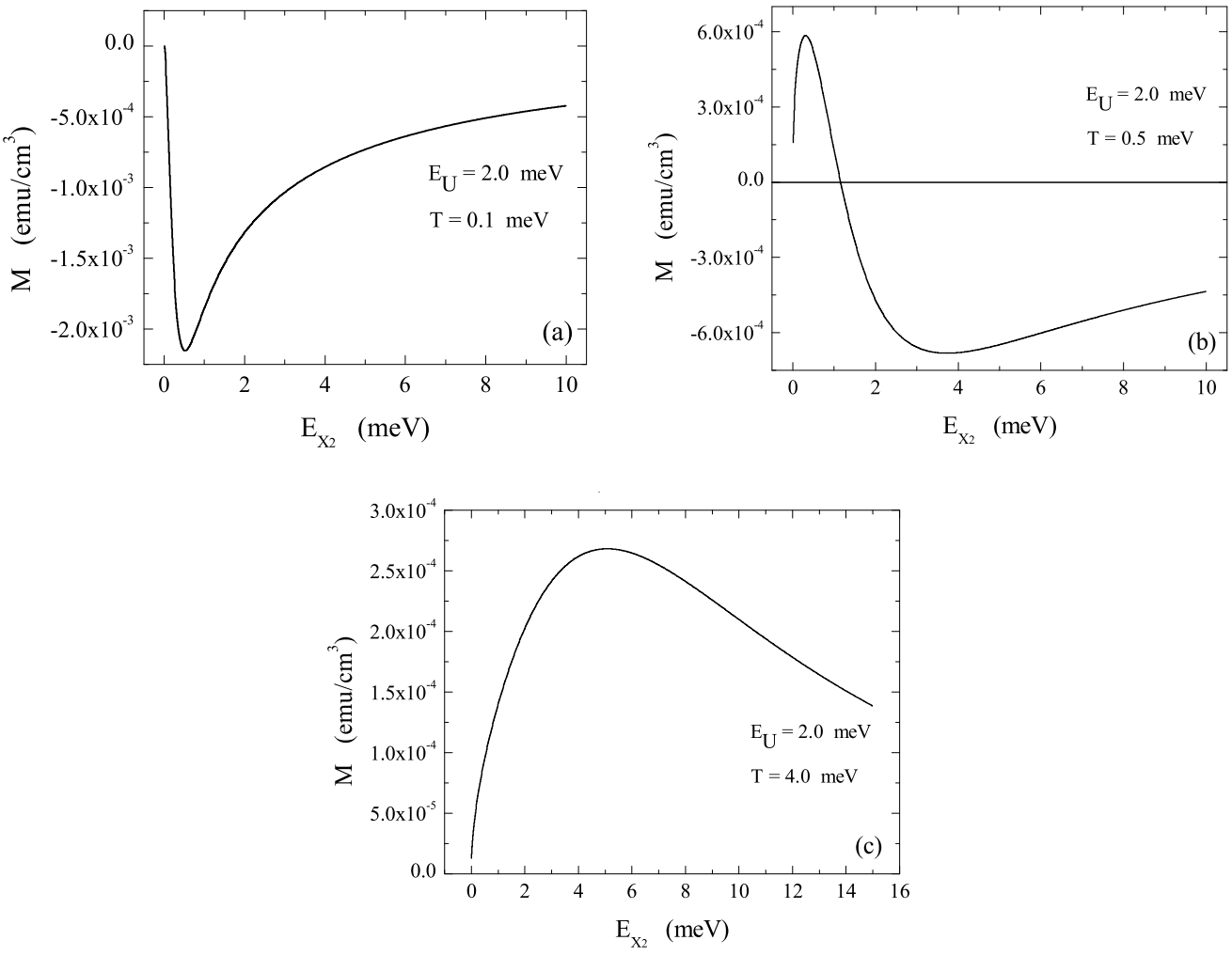

FIG. 6: Fluctuation magnetization in the first dot vs crossover parameter E_{X_2} in the second dot for different values of temperature. The fluctuation magnetization is diamagnetic for low T and paramagnetic for high T.

orbital flux through the second quantum dot. This is in contrast to the behavior of a single superconducting quantum dot for which T_c decreases monotonically as a function of orbital flux.

These counterintuitive phenomena can be understood in terms of the following cartoon picture. One can think of the two dots as two sites, each capable of containing a large number of bosons (the fluctuating pairs). The BCS pairing interaction occurs only on the first site. When there is no magnetic flux, hopping delocalizes the bosons between the two sites, leading to a "dilution" of the BCS attraction and a low critical temperature. The effect

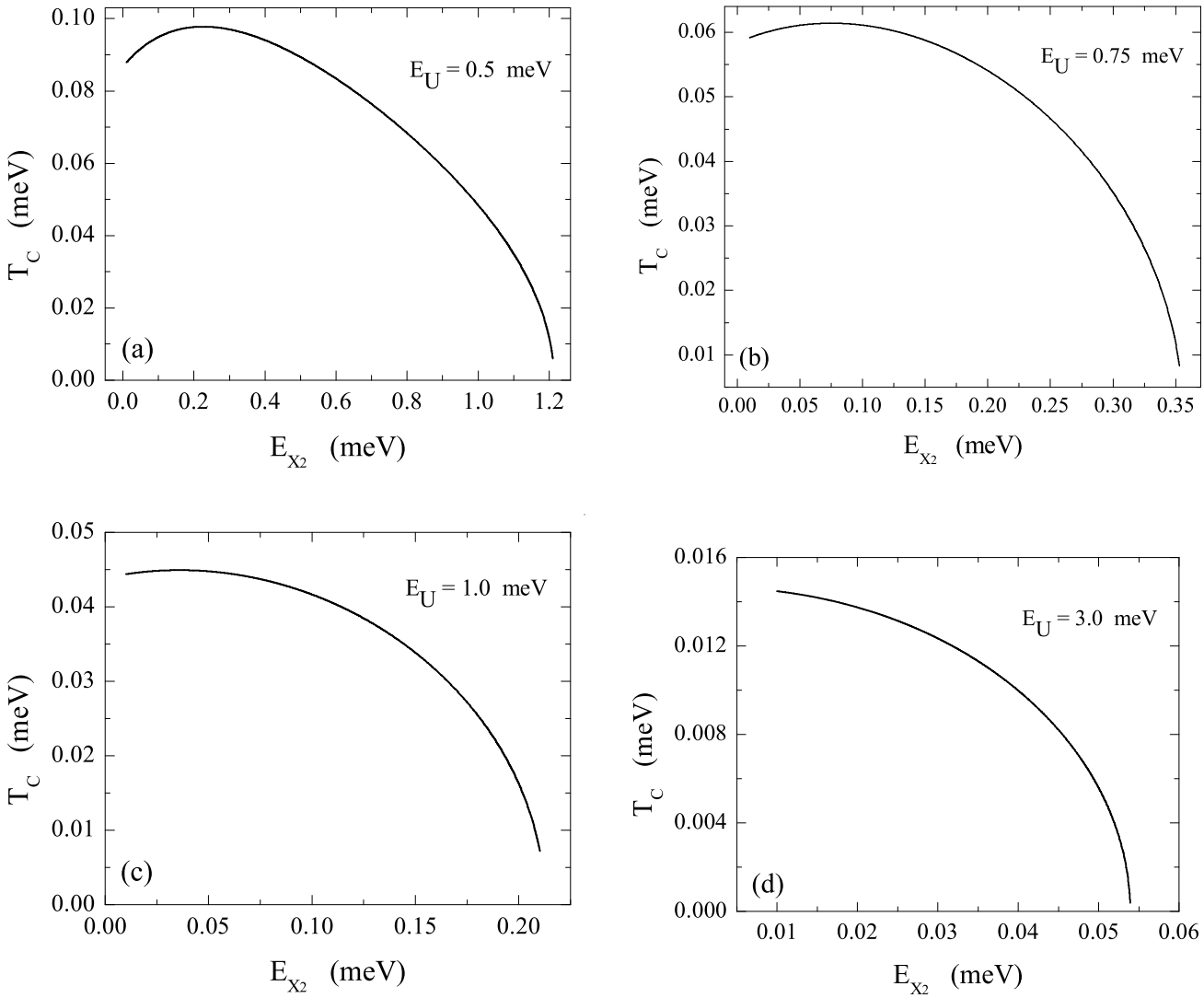

FIG. 7: Critical temperature as a function of E_{X_2} for several intermediate to strong values (compared to T_{c0}) of the hopping parameter E_U. For larger values of E_{X_2} (not shown on graphs) critical temperature is equal to zero.

of the magnetic flux on the second dot is twofold: (i) Firstly, it gaps the cooperon of the second dot, which we think of as raising the energy for the bosons to be in the second dot. (ii) Secondly, by virtue of the interdot hopping, a small time-reversal symmetry breaking is produced in the first dot, thereby raising the energy of the bosons there as well. As the flux through the second dot rises, the bosons prefer to be in the first dot since they have lower energy there. The more localized the cooper pairs are in the first dot due to effect (i), the more "undiluted" will be the effect of the BCS attraction λ, and the more favored will

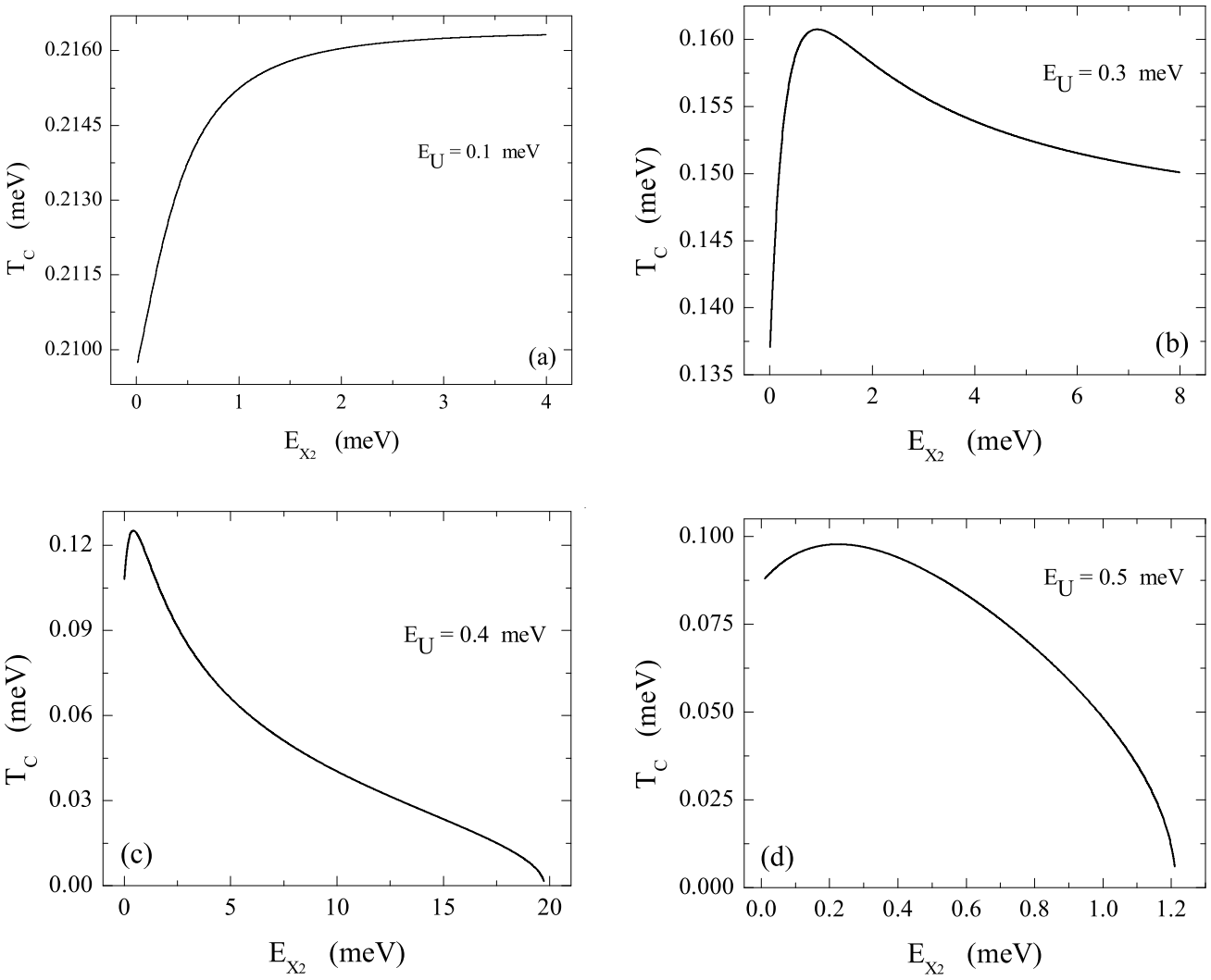

FIG. 8: Behavior of critical temperature T_C as a function of E_{X_2} for small to intermediate values (compared to T_{c0}) of E_U.

be the superconducting state. However, effect (ii) produces a time-reversal breaking in the first dot, thus disfavoring the superconducting state. These two competing effects lead to the varying behaviors of T_c and the fluctuation magnetization versus the orbital flux in the second quantum dot. When the hopping between the quantum dots is weak ($E_U < T_{c0}$), the first effect dominates, and T_c increases with E_{X_2}. When the hopping is stronger ($E_U \simeq T_{c0}$) the first effect dominates at small orbital flux, and the second at large orbital flux. Finally, at very large hopping ($E_U \gg T_{c0}$), effect (ii) is always dominant.

When considering the magnetization one must take into account the temperature as

well, so the picture is more complex. The general feature is that effect (i) which tends to localize the pairs in the first dot also tends to *decrease* the interacting free energy of the system, which leads to a paramagnetic fluctuation magnetization. Effect (ii), which breaks time-reversal in the first dot, increases the free energy of the system and thus leads to a diamagnetic fluctuation magnetization. Based on our results we infer that at high temperature the coherence of pair hopping is destroyed leading to more localization in the first quantum dot. The consequences of high T are thus similar to that of the effect (i): A lowering of the interacting free energy and a paramagnetic fluctuation magnetization.

We can make this picture a bit more quantitative for the behavior of T_c with respect to E_X. Consider once more the scaling function of Eq. (40), which we reproduce here for the reader's convenience

$$f_n(E_{X_2}, E_U, T) = \frac{E_U}{2E_1}\frac{E_{X_2}^2 + E_U E_{X_2} - E_1^2}{E_2^2 - E_1^2}\ln\left[\frac{4(\hbar\omega_D)^2 + \omega_n^2}{C'/\beta^2 + (E_1 + |\omega_n|)^2}\right] + \frac{E_U}{2E_2}\frac{E_2^2 - E_{X_2}^2 - E_U E_{X_2}}{E_2^2 - E_1^2}\ln\left[\frac{4(\hbar\omega_D)^2 + \omega_n^2}{C'/\beta^2 + (E_2 + |\omega_n|)^2}\right]. \quad (43)$$

It is straightforward to show that f_n reaches its maximum value for $\omega_n = 0$. The condition for T_c is then

$$\tilde{\lambda} f_0(E_{X_2}, E_U, T_c) = 1 \quad (44)$$

Let us first set $E_{X_2} = 0$. Let us also call the mean-field critical temperature of the *isolated* first dot in the absence of a magnetic flux T_{c0} (recall that for the parameters pertinent to Al, $T_{c0} = 0.218meV = 2.6K$). Now there are two possible limits, either $E_U \ll T_{c0}$ or $E_U \gg T_{c0}$. In the first case we obtain

$$T_c(E_U) \simeq T_{c0}\left(1 - \frac{E_U^2}{\tilde{\lambda} C' T_{c0}^2} + \cdots\right) \quad (45)$$

In the second case, $E_U \gg T_{c0}$, we obtain

$$T_c(E_U) \simeq T_{c0}\frac{\omega_D}{E_U} e^{-1/\tilde{\lambda}} \quad (46)$$

Note that this can be much smaller than T_{c0} and is an illustration of the "dilution" of the BCS attraction due to the second dot mentioned earlier. Of course, there will be a smooth crossover between the expressions of Eq. (45) and Eq. (46), so that T_c is always smaller than T_{c0}.

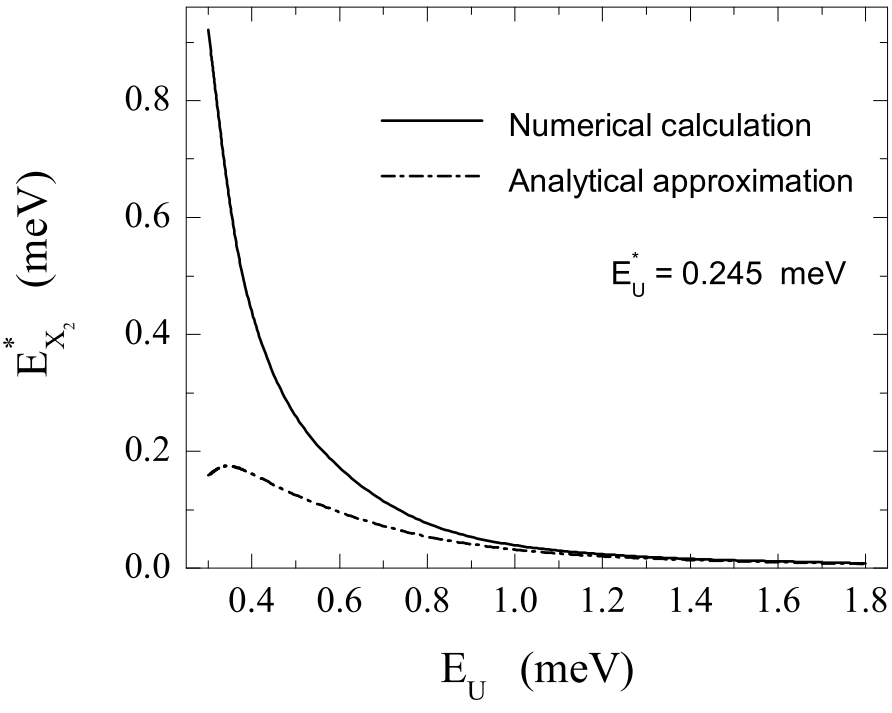

FIG. 9: The behavior of $E^*_{X_2}$ vs E_U for numerical simulation and analytical approximation.

Now under the assumption $E_{X_2},\ T_c \ll E_U$ we can solve analytically for T_c to obtain

$$T_c^2(E_{X_2}, E_U) \simeq -\frac{E_{X_2}^2}{4C'} + \frac{4\omega_D^4}{C'^2 E_U^2} e^{-4/\tilde{\lambda}} e^{\frac{2E_{X_2}}{E_U}\left(\frac{1}{\tilde{\lambda}} - \frac{1}{4} - \ln\frac{\omega_D}{E_U}\right)} \tag{47}$$

One can further find the maximum of this expression. It turns out that E_U has to be larger than a critical value E_U^* for there to be a maximum.

$$E_U^* = \omega_D e^{(\frac{1}{4} - \frac{1}{\tilde{\lambda}})} \tag{48}$$

For our values of the parameters $\omega_D = 34meV$, $\tilde{\lambda} = 0.193$, we find $E_U^* = 0.245meV$. The position of the maximum can now be estimated asymptotically for $E_U > E_U^*$ as

$$E^*_{X_2} \simeq 16e^{-1} E_U^* \left(\frac{E_U^*}{E_U}\right)^3 \ln\frac{E_U}{E_U^*} \tag{49}$$

Fig.9 compares the dependence of $E^*_{X_2}$ vs E_U in case of numerical simulation and the one described by Eq. (49). For large values of E_U compared to E_U^* the numerically computed curve matches the analytical approximation.

V. CONCLUSION AND DISCUSSION

In writing this paper we began with two objectives. We intended to compute noninteracting scaling functions in the GOE→GUE crossover in a system of two dots coupled by hopping, and to use this information to investigate the properties of an interacting system[23,24,25,26] in the many-body quantum critical regime[36,37,38].

We have considered a system of two coupled quantum dots, each of which could have its own time-reversal breaking parameter, coupled by a bridge which could also have time-reversal breaking. For each crossover parameter, there is a corresponding crossover energy scale, which represents the inverse of the time needed for the electron to "notice" the presence of that coupling in the Hamiltonian. We have computed the two-particle Green's functions in the coupled system in a large-N approximation[12], valid when all energies of interest are much greater than the mean level spacing. This allows us to compute the correlations of products of four wavefunctions belonging to two different energy levels (which have been previously calculated for a single dot for the pure ensembles by Mirlin using supersymmetry methods[50], and for the Orthogonal to Unitary crossover by Adam *et al*[23]). The two-particle Green's function splits naturally into a diffuson part and a cooperon part. Each of these parts can be represented as $\frac{1}{-i\omega}$ times a scaling function, where ω represents the frequency at which the measurement is being performed. For example, when we use the two-particle Green's function to find the ensemble average of four wavefunctions belonging to two energies, ω is the energy difference between the two states. The "scaling" nature of the scaling function is represented by the fact that it depends only on the ratio of ω to certain crossover energy scales. For the diffuson part the crossover energy E_U is controlled solely by the strength of the hopping between the two dots, while the scaling function for the cooperon part depends sensitively on the time-reversal breaking in all three parts of the system.

In the second part of the paper, we consider the case when one of the dots has an attractive BCS interaction, implying that it would be superconducting in the mean-field limit at zero temperature if it were isolated, and the other dot has no electron interactions but is penetrated by an orbital magnetic flux. The BCS interaction is one part of the Universal Hamiltonian[27,28,29,30], known to be the correct low-energy effective theory[31,32,33] in the renormalization group[34,35] sense for weak-coupling and deep within the Thouless band $|\varepsilon - \varepsilon_F| \ll E_T$. In order to eliminate complications arising from the charging energy,

we consider a particular geometry with the dots being vertically coupled and very close together in the vertical direction, as shown in Fig. 1. Our focus is on the quantum critical regime[36,37,38], achieved by increasing either the temperature or the orbital flux through the second dot. The first dot is coupled by spin-conserving hopping to a second dot on which the electrons are noninteracting. This coupling always reduces the critical temperature, due to the "diluting" effect of the second dot, that is, due to the fact that the electrons can now roam over both dots, while only one of them has a BCS attraction. Thus, the mean-field critical temperature T_c of the coupled system is always less than that of the isolated single superconducting dot T_{c0}. This part of the phenomenology is intuitively obvious.

However, when the hopping crossover energy E_U is either weak or of intermediate strength compared to T_{c0}, turning on an orbital flux in the second dot can lead to a counterintuitive *increase* in the mean-field critical temperature of the entire system. For very weak hopping, the mean-field T_c monotonically increases with orbital flux through the second dot, reaching its maximum when the second dot is fully time-reversal broken. For intermediate hopping strength, the mean-field T_c initially *increases* with increasing orbital flux to a maximum. Eventually, as the orbital flux, and therefore the crossover energy corresponding to time-reversal breaking in the second dot increases, the critical temperature once again decreases. For strong hopping $E_U \gg T_{c0}$, T_c monotonically decreases as a function of the orbital flux in the second quantum dot.

We have obtained the detailed dependence of the fluctuation magnetization in the quantum critical regime as a function of the dimensionless parameters T/E_{X_2} and E_{X_2}/E_U. Once again, the coupled dot system behaves qualitatively differently from the single dot in having a *paramagnetic* fluctuation magnetization in broad regimes of T, E_{X_2}, and E_U.

We understand these phenomena qualitatively as the result of two competing effects of the flux through the second dot. The first effect is to raise the energy for Cooper pairs in the second dot, thereby tending to localize the pairs in the first dot, and thus reducing the "diluting" effect of the second dot. This first effect tends to lower the interacting free energy (as a function of orbital flux) and raise the critical temperature. The second effect is that as the electrons hop into the second dot and return they carry information about time-reversal breaking into the first dot, which tends to increase the free energy (as a function of orbital flux) decrease the critical temperature. The first effect dominates for weak hopping and/or high T, while the second dominates for strong hopping and/or low T. Intermediate

regimes are more complex, and display nonmonotonic behavior of T_c and the fluctuation magnetization.

It should be emphasized that the quantum critical regime we focus on is qualitatively different from other *single-particle* random matrix ensembles applicable to a normal mesoscopic system which is gapless despite being in contact with one or more superconducting regions[43,44], either because the two superconductors have a phase difference of π in their order parameters[43], or because they are d-wave gapless superconductors[44]. The main difference is that we investigate and describe an interacting regime, not a single-particle one. Without the interactions there would be no fluctuation magnetization.

Let us consider some of the limitations of our work. The biggest limitation of the noninteracting part of the work is that we have used the large-N approximation, which means that we cannot trust our results when the energy scales and/or the frequency of the measurement becomes comparable to the mean level spacing. When $\omega \simeq \delta$ the wavefunctions and levels acquire correlations in the crossover which we have neglected. Another limitation is that we have used a particular model for the interdot hopping which is analytically tractable, and is modelled by a Gaussian distribution of hopping amplitudes. This might be a realistic model in vertically coupled quantum dots, or where the bridge has a large number of channels, but will probably fail if the bridge has only a few channels. These limitations could conceivably be overcome by using supersymmetric methods[14,18].

Coming now to the part of our work which deals with interactions, we have restricted ourselves to the quantum critical regime of the system, that is, when there is no mean-field BCS gap. Of course, a finite system cannot undergo spontaneous symmetry-breaking. However, in mean-field, one still finds a static BCS gap. The paradox is resolved by considering phase fluctuations of the order parameter which restore the broken symmetry[48]. To systematically investigate this issue one needs to analyze the case when the bosonic auxiliary field σ in the coupled-dot system acquires a mean-field expectation value and quantize its phase fluctuations.

We have also chosen a geometry in which interdot charging effects can be ignored. However, most experimental systems with superconducting nanoparticles deal with almost spherical particles. For two such nanoparticles coupled by hopping, one cannot ignore charging effects[24,39,40,41]. We expect these to have a nontrivial effect on the mean-field T_c and fluctuation magnetization of the combined system. We defer this analysis to future work.

There are several other future directions in which this work could be extended. New symmetry classes[51,52] have been discovered recently for two-dimensional disordered/ballistic-chaotic systems subject to spin-orbit coupling[53,54]. In one of these classes, the spin-orbit coupling is unitarily equivalent to an orbital flux acting oppositely[51,52] on the two eigenstates of a single-particle quantum number algebraically identical to σ_z. Due to the unitary transformation, this quantum number has no simple interpretation in the original (Orthogonal) basis. However, it is clear that the results of this paper could be applied, *mutatis mutandis*, to two coupled two-dimensional quantum dots subject to spin-orbit couplings. In particular, consider the situation where one quantum dot has no spin-orbit coupling, but does have a Stoner exchange interaction, while the other dot is noninteracting, but is made of a different material and has a strong spin-orbit coupling. Work by one of us has shown[26] that by tuning the spin-orbit coupling one can access the quantum critical regime, which is dominated by many-body quantum fluctuations. The above configuration offers a way to continuously tune the spin-orbit coupling in the first dot by changing the strength of the hopping between the dots.

In general, one can imagine a wide range of circumstances where changing a crossover parameter in one (noninteracting) dot allows one to softly and tunably break a symmetry in the another (interacting) dot, thereby allowing one access to a quantum critical regime. We hope the present work will be useful in exploring such phenomena.

Acknowledgments

The authors would like to thank National Science Foundation for partial support under DMR-0311761, and Yoram Alhassid for comments on the manuscript. OZ wishes to thank the College of Arts and Sciences and the Department of Physics at the University of Kentucky for partial support. The authors are grateful to O. Korneta for technical help with graphics.

APPENDIX A: ONE UNCOUPLED DOT

In this Appendix we calculate one-particle and two-particle Green's functions for a single dot undergoing the crossover. The strength of magnetic field inside the dot is controlled by crossover parameter X. The Hamiltonian of the system in crossover is:

$$H = \frac{H_S + iXH_A}{\sqrt{1+X^2}}, \tag{A1}$$

where $H_{S,A}$ are symmetric and antisymmetric real random matrices with the same variance for matrix elements. Normalization $(1+X^2)^{-1/2}$ keeps the mean level spacing δ fixed as magnetic field changes inside the dot.

We define the retarded one-particle Green's function as follows:

$$G^R_{\alpha\beta}(E) = \left(\frac{1}{E^+ - H}\right)_{\alpha\beta} = \frac{1}{E^+}\left(I + \frac{H}{E^+} + \frac{H^2}{(E^+)^2} + \dots\right)_{\alpha\beta} = \frac{\delta_{\alpha\beta}}{E^+} + \frac{H_{\alpha\beta}}{(E^+)^2} + \frac{H^2_{\alpha\beta}}{(E^+)^3} + \dots, \tag{A2}$$

Here H is a Hamiltonian, and E^+ is the energy with infinitely small positive imaginary part $E^+ = E + i\eta$.

This series has nice graphical representation:

$G^R(E)$ = 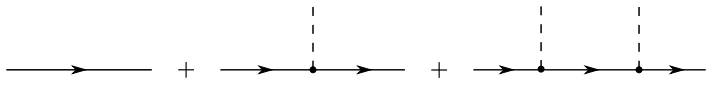 + ..., (A3)

where straight solid line represents $1/E^+$ and dashed line stands for Hamiltonian.

$\frac{1}{E^+}$ = , H = (A4)

Just as in disordered conductor or quantum field theory the target is not the Green's function itself, but rather its mean and mean square. We take on random matrix ensemble average of $G_{\alpha\beta}$. Such averaging assumes knowledge of $\langle H^n \rangle$, where angular brackets stand for gaussian ensemble averaging, and $n = 1, \infty$. For $n = 1$ we have $\langle H \rangle = 0$, while for $n = 2$ the second moment reads:

$$\langle H_{\alpha\gamma} H_{\delta\beta} \rangle = \frac{\langle H^s_{\alpha\gamma} H^s_{\delta\beta} \rangle - X^2 \langle H^a_{\alpha\gamma} H^a_{\delta\beta} \rangle}{1+X^2} = \frac{N\delta^2}{\pi^2}\delta_{\alpha\beta}\delta_{\gamma\delta} + \left(\frac{1-X^2}{1+X^2}\right)\frac{N\delta^2}{\pi^2}\delta_{\alpha\delta}\delta_{\gamma\beta}. \tag{A5}$$

All higher moments of H can be computed using Wick's theorem[55]. Thus, the ensemble averaging leaves only the terms containing even moments of H. Introducing the notation for $\langle HH \rangle =$  , we obtain, for the averaged G^R series:

$\langle G^R(E) \rangle$ = 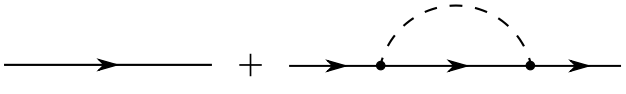 + ... (A6)

Then, the expansion (A6) can be written in a compact form of Dyson equation:

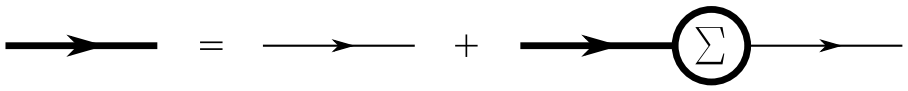

(A7)

The bold line denotes the full one-particle Green's function averaged over Gaussian ensemble, and Σ is a self-energy, representing the sum of all topologically different diagrams. The corresponding algebraic expression for the Dyson equation can be easily extracted from Eq. (A7) producing:

$$G_{\alpha\beta} = \sum_{\nu\mu} G_{\alpha\nu}\Sigma_{\nu\mu}\frac{\delta_{\mu\beta}}{E^+} + \frac{\delta_{\alpha\beta}}{E^+}, \tag{A8}$$

where $G_{\alpha\beta}$ means $\langle G^R_{\alpha\beta}(E)\rangle$. Now, using the fact that $G_{\alpha\beta} = G_\alpha\delta_{\alpha\beta}$ and $\Sigma_{\alpha\beta} = \Sigma_\alpha\delta_{\alpha\beta}$ (no summation over α implied), one can solve this equation and obtain:

$$G_{\alpha\beta} = \frac{\delta_{\alpha\beta}}{E^+ - \Sigma}. \tag{A9}$$

Next we approximate self-energy by the first term in large N approximation:

$$\Sigma_{\alpha\beta} = \quad = G\sum_\gamma \langle H_{\alpha\gamma}H_{\gamma\beta}\rangle \approx \left(\frac{N\delta}{\pi}\right)^2 \frac{\delta_{\alpha\beta}}{E^+ - \Sigma}. \tag{A10}$$

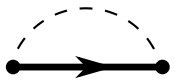

Solving Eq. (A10) for the self-energy we determine:

$$\Sigma = \frac{E}{2} - \frac{i}{2}\sqrt{\left(\frac{2N\delta}{\pi}\right)^2 - E^2}. \tag{A11}$$

Consequently, the ensemble average of one-particle Green's function is given by:

$$\langle G^R_{\alpha\beta}(E)\rangle = \frac{\delta_{\alpha\beta}}{\frac{E}{2} + \frac{i}{2}\sqrt{\left(\frac{2N\delta}{\pi}\right)^2 - E^2}}; \qquad \langle G^A_{\alpha\beta}(E)\rangle = \langle G^R_{\beta\alpha}(E)\rangle^*. \tag{A12}$$

Next, to study the two-particle Green's function we notice that the main contributions come from ladder and maximally crossed diagrams:

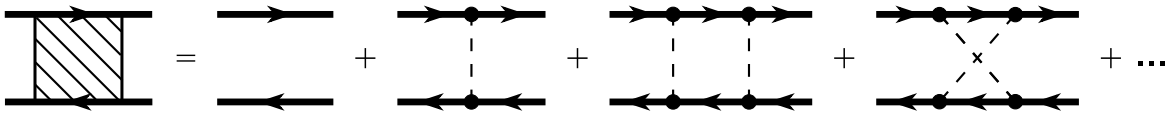

(A13)

Two bold lines on the left side stand for the average two-particle Green's function $\langle G^R(E+\omega)G^A(E)\rangle$. The sum of ladder diagrams is described by Bethe-Salpeter equation:

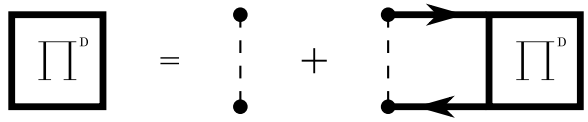

(A14)

or,

$$\Pi^{\alpha\beta,D}_{\delta\gamma} = \frac{N\delta^2}{\pi^2}\delta_{\alpha\delta}\delta_{\beta\gamma} + \left(\frac{N\delta}{\pi}\right)^2 \frac{\Pi^{\alpha\beta,D}_{\delta\gamma}}{F[E,\omega]}, \tag{A15}$$

where Π^D is a ladder approximation of diffuson part of two-particle Green's function. Here $F[E,\omega]$ is a product of two inversed averaged one-particle Green's functions and in the limit $\omega \ll N\delta$ is:

$$F[E,\omega] = \langle G^R(E+\omega)\rangle^{-1}\langle G^A(E)\rangle^{-1} \approx -\frac{i\omega\delta N}{2\pi} + \left(\frac{N\delta}{\pi}\right)^2. \tag{A16}$$

One can solve this equation taking into account $\Pi^{\alpha\beta,D}_{\delta\gamma} = \Pi^D\delta_{\alpha\delta}\delta_{\beta\gamma}$:

$$\Pi^D = \frac{N\delta^2}{\pi^2}\frac{F[E,\omega]}{F[E,\omega] - \left(\frac{N\delta}{\pi}\right)^2}. \tag{A17}$$

Multiplying Π^D by $F^2[E,\omega]$ we arrive at the following expression for the diffuson term:

$$\langle G^R_{\alpha\gamma}(E+\omega)G^A_{\delta\beta}(E)\rangle_D = \frac{2\pi}{N^2\delta}\frac{\delta_{\alpha\beta}\delta_{\gamma\delta}}{-i\omega}. \tag{A18}$$

Then, we turn our attention to the equation for maximally crossed diagrams. We have

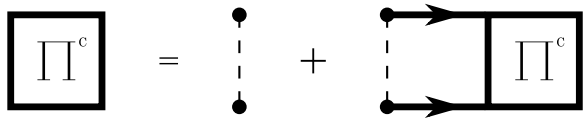

(A19)

and Π^C is expressed in terms of $F[E,\omega]$ again:

$$\Pi^C = \left(\frac{1-X^2}{1+X^2}\right)\frac{N\delta^2}{\pi^2}\frac{F[E,\omega]}{F[E,\omega] - \frac{1-X^2}{1+X^2}\left(\frac{N\delta}{\pi}\right)^2}. \tag{A20}$$

Assuming X to be small compared to unity (weak crossover), we evaluate the contribution of maximally crossed diagrams to Green's function to get:

$$\langle G^R_{\alpha\gamma}(E+\omega)G^A_{\delta\beta}(E)\rangle_C = \frac{2\pi}{N^2\delta}\frac{\delta_{\alpha\delta}\delta_{\gamma\beta}}{-i\omega}\frac{1}{1+i\frac{E_X}{\omega}}, \tag{A21}$$

where $E_X = 4X^2 N\delta/\pi$ is a crossover energy scale. Final expression for the connected part of the two-particle Green's function is:

$$\langle G^R_{\alpha\gamma}(E+\omega) G^A_{\delta\beta}(E)\rangle = \frac{2\pi}{N^2\delta}\frac{\delta_{\alpha\beta}\delta_{\gamma\delta}}{-i\omega} + \frac{2\pi}{N^2\delta}\frac{\delta_{\alpha\delta}\delta_{\gamma\beta}}{-i\omega}\frac{1}{1+i\frac{E_X}{\omega}}. \tag{A22}$$

APPENDIX B: TWO COUPLED DOTS

This Appendix contains details of the derivation for statistical properties of the Green's functions for the two coupled dots connected to each other via hopping bridge V. Coupling between dots is weak and characterized by dimensionless parameter U. For the system of uncoupled dots the Hilbert space is a direct sum of spaces for dot 1 and dot 2. Hopping V mixes the states from two spaces. The Hamiltonian of the system can be represented as:

$$H_{tot} = \begin{pmatrix} H_1 & V \\ V^\dagger & H_2 \end{pmatrix}. \tag{B1}$$

For $H_{1,2}$ and V we have:

$$H_n = \frac{H_n^S + iX_n H_n^A}{\sqrt{1+X_n^2}},\ i=1,2; \qquad V = \frac{V^R + i\Gamma V^I}{\sqrt{1+\Gamma^2}}. \tag{B2}$$

Here S (A) stands for symmetric (antisymmetric), and R (I) means real (imaginary). Below we use Greek indices for dot 1, and Latin indices for dot 2. We also found it convenient to keep bandwidth of both dots the same; that is, $N_1\delta_1 = N_2\delta_2$ with $\xi = \delta_1/\delta_2$.

The following averaged products of matrix elements of H can be obtained:

$$\begin{aligned} \langle H_{\alpha\gamma} H_{\delta\beta}\rangle &= \frac{N_1\delta_1^2}{\pi^2}\delta_{\alpha\beta}\delta_{\gamma\delta} + \left(\frac{1-X_1^2}{1+X_1^2}\right)\frac{N_1\delta_1^2}{\pi^2}\delta_{\alpha\delta}\delta_{\gamma\beta} \\ \langle H_{il} H_{kj}\rangle &= \frac{N_2\delta_2^2}{\pi^2}\delta_{ij}\delta_{lk} + \left(\frac{1-X_2^2}{1+X_2^2}\right)\frac{N_2\delta_2^2}{\pi^2}\delta_{ik}\delta_{lj}, \end{aligned} \tag{B3}$$

where X_1 and X_2 are the crossover parameters in dot 1 and 2. Pairings between V matrix elements are:

$$\begin{aligned} \langle V_{\alpha i} V_{\beta j}\rangle = \langle V^\dagger_{i\alpha} V^\dagger_{j\beta}\rangle &= \left(\frac{1-\Gamma^2}{1+\Gamma^2}\right)\frac{\sqrt{N_1 N_2}\delta_1\delta_2 U}{\pi^2}\delta_{\alpha\beta}\delta_{ij} \\ \langle V_{\alpha i} V^\dagger_{j\beta}\rangle &= \frac{\sqrt{N_1 N_2}\delta_1\delta_2 U}{\pi^2}\delta_{\alpha\beta}\delta_{ij}, \end{aligned} \tag{B4}$$

with Γ a crossover parameter in hopping bridge. Normalization for V pairing is chosen to coincide with that of $\langle HH\rangle$ when $\xi = 1$.

To determine one-particle Green's function we use the system listed in Eq. (20). The straight and wavy bold lines with arrows represent averaged functions $\langle G_1^R(E)\rangle$, $\langle G_2^R(E)\rangle$ in dot 1 and 2, regular lines represent bare propagators, and the rest of the lines describe pairings between H_{tot} matrix elements. We have:

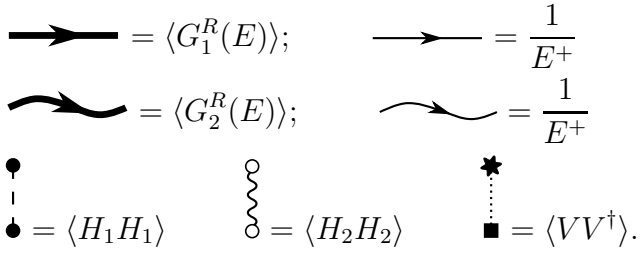

(B5)

The corresponding analytical expressions of this system of equations are:

$$G_1 = \frac{\Sigma^{11} G_1}{E^+} + \frac{\Sigma^{12} G_1}{E^+} + \frac{1}{E^+}$$
$$G_2 = \frac{\Sigma^{22} G_2}{E^+} + \frac{\Sigma^{21} G_2}{E^+} + \frac{1}{E^+},$$

with G_1 and G_2 connected to Green's functions via: $\langle G^R_{\alpha\gamma,1}(E)\rangle = G_1\delta_{\alpha\gamma}$, $\langle G^R_{il,2}(E)\rangle = G_2\delta_{il}$ The self-energies Σ^{nm} are to be determined using standard procedure[14].

We observe, that the system of two linear equations (B) has a solution:

$$G_1 = \frac{1}{E^+ - \Sigma^{11} - \Sigma^{12}}, \qquad G_2 = \frac{1}{E^+ - \Sigma^{22} - \Sigma^{21}}.$$

Here we approximated self-energies by the first term in large N expansion again. In this approximation evaluation of Σ^{nm} yields:

$$\Sigma^{11}_{\alpha\beta} = \Sigma^{11}\delta_{\alpha\beta} = {}^{\alpha}\!\!\;\beta = G_1 \sum_\gamma \langle H_{\alpha\gamma} H_{\gamma\beta}\rangle = \left(\frac{N_1\delta_1}{\pi}\right)^2 \frac{\delta_{\alpha\beta}}{E^+ - \Sigma^{11} - \Sigma^{12}}$$

$$\Sigma^{12}_{\alpha\beta} = \Sigma^{12}\delta_{\alpha\beta} = {}^{\alpha}\!\!\;\beta = G_2 \sum_i \langle V_{\alpha i} V^\dagger_{i\beta}\rangle = \frac{\sqrt{N_1 N_2} N_2 \delta_1 \delta_2 U}{\pi^2} \frac{\delta_{\alpha\beta}}{E^+ - \Sigma^{22} - \Sigma^{21}}$$

$$\Sigma^{22}_{ij} = i \;\; j = \left(\frac{N_2\delta_2}{\pi}\right)^2 \frac{\delta_{ij}}{E^+ - \Sigma^{22} - \Sigma^{21}}$$

$$\Sigma^{21}_{ij} = i \;\; j = \frac{\sqrt{N_1 N_2} N_1 \delta_1 \delta_2 U}{\pi^2} \frac{\delta_{ij}}{E^+ - \Sigma^{11} - \Sigma^{12}}.$$

Thus, to find all Σ^{nm} one needs to solve the following system of equations:

$$\begin{aligned}
\Sigma^{11}\left(E^{+}-\Sigma^{11}-\Sigma^{12}\right) &= \left(\frac{N_1\delta_1}{\pi}\right)^2 \\
\Sigma^{12}\left(E^{+}-\Sigma^{22}-\Sigma^{21}\right) &= \frac{\sqrt{N_1N_2}N_2\delta_1\delta_2 U}{\pi^2} \\
\Sigma^{22}\left(E^{+}-\Sigma^{22}-\Sigma^{21}\right) &= \left(\frac{N_2\delta_2}{\pi}\right)^2 \\
\Sigma^{21}\left(E^{+}-\Sigma^{11}-\Sigma^{12}\right) &= \frac{\sqrt{N_1N_2}N_1\delta_1\delta_2 U}{\pi^2}.
\end{aligned} \tag{B6}$$

Observing that $\Sigma^{21} = U\Sigma^{11}/\sqrt{\xi}$ and $\Sigma^{12} = U\sqrt{\xi}\Sigma^{11}$ we decouple the system given in Eq. (B6). For example, the pair of first and third equations can be rewritten as:

$$\begin{aligned}
(\Sigma^{11})^2 - E\Sigma^{11} + U\sqrt{\xi}\Sigma^{11}\Sigma^{22} &= -\left(\frac{N_1\delta_1}{\pi}\right)^2 \\
(\Sigma^{22})^2 - E\Sigma^{22} + \frac{U}{\sqrt{\xi}}\Sigma^{11}\Sigma^{22} &= -\left(\frac{N_2\delta_2}{\pi}\right)^2.
\end{aligned} \tag{B7}$$

For weak coupling the solution can be found by expanding self-energies Σ^{11} and Σ^{22} in series in U. Taking the solution for single dot as zero approximation (below all the solutions for the uncoupled dot will be marked with subscript 0) we get

$$\Sigma^{11} = \Sigma_0^{11} + U\Sigma_1^{11} \tag{B8}$$

$$\Sigma^{22} = \Sigma_0^{22} + U\Sigma_1^{22}. \tag{B9}$$

Note that $N_1\delta_1 = N_2\delta_2$, and $\Sigma_0^{11} = \Sigma_0^{22} \equiv \Sigma_0$.

Plugging into the right hand side of Eq. (B9) in system (B7) we arrive at:

$$\begin{aligned}
\Sigma^{11} &= \Sigma_0\left(1 + U\sqrt{\xi}\frac{\Sigma_0}{E^{+}-2\Sigma_0}\right) \\
\Sigma^{22} &= \Sigma_0\left(1 + \frac{U}{\sqrt{\xi}}\frac{\Sigma_0}{E^{+}-2\Sigma_0}\right) \\
\Sigma^{21} &= \frac{U}{\sqrt{\xi}}\Sigma^{11} \\
\Sigma^{12} &= U\sqrt{\xi}\Sigma^{22}.
\end{aligned} \tag{B10}$$

Neglecting the higher powers in U for one-particle Green's functions we finally arrive at the following expressions for the single particle Green's functions:

$$\begin{aligned}
\langle G^R_{\alpha\beta,1}(E)\rangle &= \frac{\langle G^R_{\alpha\beta,0}(E)\rangle}{1-U\sqrt{\xi}\frac{\Sigma_0}{E-2\Sigma_0}} = \frac{\delta_{\alpha\beta}}{\left(\frac{N_1\delta_1}{\pi}\right)\left[\epsilon+i\sqrt{1-\epsilon^2}\right]}\frac{1}{\left[1+\frac{U\sqrt{\xi}}{2}\left(1+i\frac{\epsilon}{\sqrt{1-\epsilon^2}}\right)\right]} \\
\langle G^R_{ij,2}(E)\rangle &= \frac{\langle G^R_{ij,0}(E)\rangle}{1-\frac{U}{\sqrt{\xi}}\frac{\Sigma_0}{E-2\Sigma_0}} = \frac{\delta_{ij}}{\left(\frac{N_2\delta_2}{\pi}\right)\left[\epsilon+i\sqrt{1-\epsilon^2}\right]}\frac{1}{\left[1+\frac{U}{2\sqrt{\xi}}\left(1+i\frac{\epsilon}{\sqrt{1-\epsilon^2}}\right)\right]},
\end{aligned}$$

where $\epsilon = \pi E/2N\delta$.

Now we switch our attention to the calculational procedure for the average of the two-particle Green's functions $\langle G^R_{\alpha\gamma,1}(E+\omega)G^A_{\delta\beta,1}(E)\rangle$ and $\langle G^R_{il,2}(E+\omega)G^A_{kj,2}(E)\rangle$. In the limit of large N_1 and N_2 ladder and maximally crossed diagrams contribute the most. For ladder diagrams we obtain the system of Bethe-Salpeter equations (see Eq. (22)). Here we used the following notation:

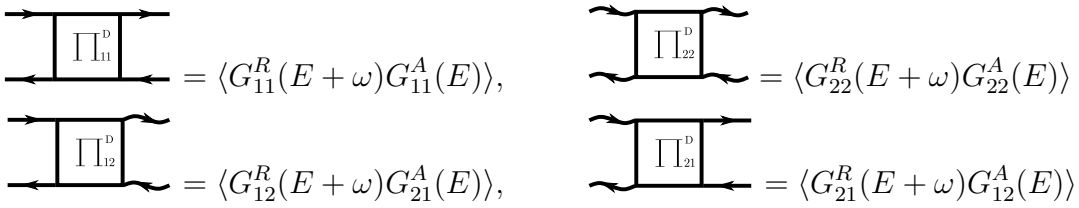

(B11)

For the diffuson Π^D_{nm} the system of algebraic equations reeds:

$$\begin{aligned}
\Pi^D_{11} &= \frac{N_1\delta_1^2}{\pi^2} + \frac{N_1\delta_1^2}{\pi^2}\frac{N_1\Pi^D_{11}}{F_1[E,\omega]} + \frac{\sqrt{N_1N_2}\delta_1\delta_2U}{\pi^2}\frac{N_2\Pi^D_{21}}{F_2[E,\omega]} \\
\Pi^D_{22} &= \frac{N_2\delta_2^2}{\pi^2} + \frac{N_2\delta_2^2}{\pi^2}\frac{N_2\Pi^D_{22}}{F_2[E,\omega]} + \frac{\sqrt{N_1N_2}\delta_1\delta_2U}{\pi^2}\frac{N_1\Pi^D_{12}}{F_1[E,\omega]} \\
\Pi^D_{12} &= \frac{\sqrt{N_1N_2}\delta_1\delta_2U}{\pi^2} + \frac{N_1\delta_1^2}{\pi^2}\frac{N_1\Pi^D_{12}}{F_1[E,\omega]} + \frac{\sqrt{N_1N_2}\delta_1\delta_2U}{\pi^2}\frac{N_2\Pi^D_{22}}{F_2[E,\omega]} \\
\Pi^D_{21} &= \frac{\sqrt{N_1N_2}\delta_1\delta_2U}{\pi^2} + \frac{N_2\delta_2^2}{\pi^2}\frac{N_2\Pi^D_{21}}{F_2[E,\omega]} + \frac{\sqrt{N_1N_2}\delta_1\delta_2U}{\pi^2}\frac{N_1\Pi^D_{11}}{F_1[E,\omega]},
\end{aligned}$$

(B12)

where $F_1[E,\omega]$ and $F_2[E,\omega]$ are defined as products of inverse averaged one-particle Green's functions in the first and second dots respectively. For small values of U and ω these functions can be approximated as follows:

$$F_1[E,\omega] = \langle G_1^R(E+\omega)\rangle^{-1}\langle G_1^A(E)\rangle^{-1} \approx \left(\frac{N_1\delta_1}{\pi}\right)^2\left[1+\sqrt{\xi}U - i\tilde{\omega}\right]$$
$$F_2[E,\omega] = \langle G_2^R(E+\omega)\rangle^{-1}\langle G_2^A(E)\rangle^{-1} \approx \left(\frac{N_2\delta_2}{\pi}\right)^2\left[1+\frac{U}{\sqrt{\xi}} - i\tilde{\omega}\right], \tag{B13}$$

where $\tilde{\omega} = \pi\omega/2N\delta$. The system of four equations given by the Eq. (B12) can be decoupled into the two systems of two equations each. To determine Π_{11}^D one solves the system of the first and the last equations of Eq. (B12) to get:

$$\begin{aligned}
&\left(1-\frac{\left(\frac{N_1\delta_1}{\pi}\right)^2}{F_1(E,\omega)}\right)\Pi_{11}^D - \frac{\sqrt{N_1N_2}N_2\delta_1\delta_2U}{\pi^2}\frac{\Pi_{21}^D}{F_2(E,\omega)} = \frac{N_1\delta_1^2}{\pi^2}\\
&\left(1-\frac{\left(\frac{N_2\delta_2}{\pi}\right)^2}{F_2(E,\omega)}\right)\Pi_{21}^D - \frac{\sqrt{N_1N_2}N_1\delta_1\delta_2U}{\pi^2}\frac{\Pi_{11}^D}{F_1(E,\omega)} = \frac{\sqrt{N_1N_2}\delta_1\delta_2U}{\pi^2}.
\end{aligned} \tag{B14}$$

Then, solving the resulting system (Eq. (B14)) and attaching external lines one obtains expression for the two-particle Green's function in dot 1:

$$\langle G^R_{\alpha\gamma,1}(E+\omega)G^A_{\delta\beta,1}(E)\rangle_D = \frac{2\pi}{N_1^2\delta_1}\frac{\delta_{\alpha\beta}\delta_{\gamma\delta}}{-i\omega}\frac{1+\frac{i}{\sqrt{\xi}}\frac{E_U}{\omega}}{1+i(\sqrt{\xi}+\frac{1}{\sqrt{\xi}})\frac{E_U}{\omega}}. \tag{B15}$$

The corresponding correlator for dot 2 is readily obtained as well:

$$\langle G^R_{il,2}(E+\omega)G^A_{kj,2}(E)\rangle_D = \frac{2\pi}{N_2^2\delta_2}\frac{\delta_{ij}\delta_{lk}}{-i\omega}\frac{1+i\sqrt{\xi}\frac{E_U}{\omega}}{1+i(\sqrt{\xi}+\frac{1}{\sqrt{\xi}})\frac{E_U}{\omega}}. \tag{B16}$$

For the second part of the Green's function (which is the sum of maximally crossed diagrams) the system of equations is described by Eq. (24). Transforming this graphical system into the algebraic one, we get:

$$\begin{aligned}
\Pi_{11}^C &= \left(\frac{1-X_1^2}{1+X_1^2}\right)\frac{N_1\delta_1^2}{\pi^2} + \left(\frac{1-X_1^2}{1+X_1^2}\right)\frac{N_1\delta_1^2}{\pi^2}\frac{N_1\Pi_{11}^C}{F_1[E,\omega]} + \left(\frac{1-\Gamma^2}{1+\Gamma^2}\right)\frac{\sqrt{N_1N_2}\delta_1\delta_2U}{\pi^2}\frac{N_2\Pi_{21}^C}{F_2[E,\omega]}\\
\Pi_{22}^C &= \left(\frac{1-X_2^2}{1+X_2^2}\right)\frac{N_2\delta_2^2}{\pi^2} + \left(\frac{1-X_2^2}{1+X_2^2}\right)\frac{N_2\delta_2^2}{\pi^2}\frac{N_2\Pi_{22}^C}{F_2[E,\omega]} + \left(\frac{1-\Gamma^2}{1+\Gamma^2}\right)\frac{\sqrt{N_1N_2}\delta_1\delta_2U}{\pi^2}\frac{N_1\Pi_{12}^C}{F_1[E,\omega]}\\
\Pi_{12}^C &= \left(\frac{1-\Gamma^2}{1+\Gamma^2}\right)\frac{\sqrt{N_1N_2}\delta_1\delta_2U}{\pi^2} + \left(\frac{1-\Gamma^2}{1+\Gamma^2}\right)\frac{\sqrt{N_1N_2}\delta_1\delta_2U}{\pi^2}\frac{N_2\Pi_{22}^C}{F_2[E,\omega]} + \left(\frac{1-X_1^2}{1+X_1^2}\right)\frac{N_1\delta_1^2}{\pi^2}\frac{N_1\Pi_{12}^C}{F_1[E,\omega]}\\
\Pi_{21}^C &= \left(\frac{1-\Gamma^2}{1+\Gamma^2}\right)\frac{\sqrt{N_1N_2}\delta_1\delta_2U}{\pi^2} + \left(\frac{1-\Gamma^2}{1+\Gamma^2}\right)\frac{\sqrt{N_1N_2}\delta_1\delta_2U}{\pi^2}\frac{N_1\Pi_{11}^C}{F_1[E,\omega]} + \left(\frac{1-X_2^2}{1+X_2^2}\right)\frac{N_2\delta_2^2}{\pi^2}\frac{N_2\Pi_{21}^C}{F_2[E,\omega]}.
\end{aligned} \tag{B17}$$

Once again, the system at hand breaks into systems of two equations each. We proceed by combining the first and the last equations to obtain:

$$\left[1-\left(\frac{1-X_1^2}{1+X_1^2}\right)\frac{\left(\frac{N_1\delta_1}{\pi}\right)^2}{F_1[E,\omega]}\right]\Pi_{11}^C-\left(\frac{1-\Gamma^2}{1+\Gamma^2}\right)\frac{\sqrt{N_1N_2}N_2\delta_1\delta_2U}{\pi^2}\frac{\Pi_{21}^C}{F_2[E,\omega]}=\left(\frac{1-X_1^2}{1+X_1^2}\right)\frac{N_1\delta_1^2}{\pi^2}$$
$$-\left(\frac{1-\Gamma^2}{1+\Gamma^2}\right)\frac{\sqrt{N_1N_2}N_1\delta_1\delta_2U}{\pi^2}\frac{\Pi_{11}^C}{F_1[E,\omega]}+\left[1-\left(\frac{1-X_2^2}{1+X_2^2}\right)\frac{\left(\frac{N_2\delta_2}{\pi}\right)^2}{F_2[E,\omega]}\right]\Pi_{21}^C=\left(\frac{1-\Gamma^2}{1+\Gamma^2}\right)\frac{\sqrt{N_1N_2}\delta_1\delta_2U}{\pi^2}. \tag{B18}$$

Now we can construct approximations for the expressions, containing crossover parameters. For example, for small values of X and Γ the solution for Π_{11}^C is expressed as follows:

$$\Pi_{11}^C=\frac{N_1\delta_1^2}{\pi^2}\frac{(1-2X_1^2)(\frac{U}{\sqrt{\xi}}-i\tilde{\omega}+2X_2^2)+(1-4\Gamma^2)U^2}{(\sqrt{\xi}U-i\tilde{\omega}+2X_1^2)(\frac{U}{\sqrt{\xi}}-i\tilde{\omega}+2X_2^2)-(1-4\Gamma^2)U^2}. \tag{B19}$$

Next, introducing crossover energy scales:

$$E_X=4X^2\frac{N\delta}{\pi}\qquad E_U=2U\frac{N\delta}{\pi}\qquad E_\Gamma=\frac{4\Gamma^2E_U}{\sqrt{\xi}+\frac{1}{\sqrt{\xi}}} \tag{B20}$$

we obtain the solution for Π_{11}^C in the following form:

$$\Pi_{11}^C=\frac{N_1\delta_1^2}{\pi^2}\frac{1}{-i\tilde{\omega}}\frac{1-\frac{E_U}{\sqrt{\xi}i\omega}-\frac{E_{X_2}}{i\omega}}{1-\frac{E_{X_1}+E_{X_2}}{i\omega}+\frac{E_{X_1}E_{X_2}}{(i\omega)^2}+\frac{E_{X_1}E_U}{\sqrt{\xi}(i\omega)^2}+\frac{\sqrt{\xi}E_{X_2}E_U}{(i\omega)^2}+\left(\sqrt{\xi}+\frac{1}{\sqrt{\xi}}\right)\frac{E_U}{i\omega}\left(\frac{E_\Gamma}{i\omega}-1\right)}. \tag{B21}$$

Then, adding external lines to Π_{11}^C for Green's function we get:

$$\langle G^R_{\alpha\gamma,1}(E+\omega)G^A_{\delta\beta,1}(E)\rangle_C=$$
$$\frac{2\pi}{N_1^2\delta_1}\frac{\delta_{\alpha\delta}\delta_{\gamma\beta}}{-i\omega}\frac{1+\frac{i}{\sqrt{\xi}}\frac{E_U}{\omega}+i\frac{E_{X_2}}{\omega}}{1+i\frac{E_{X_1}+E_{X_2}}{\omega}-\frac{E_{X_1}E_{X_2}}{\omega^2}-\frac{E_{X_1}E_U}{\sqrt{\xi}\omega^2}-\frac{\sqrt{\xi}E_{X_2}E_U}{\omega^2}+i\left(\sqrt{\xi}+\frac{1}{\sqrt{\xi}}\right)\frac{E_U}{\omega}\left(1+i\frac{E_\Gamma}{\omega}\right)}. \tag{B22}$$

Similar manipulations for the corresponding correlator of Green's functions for the second room result in:

$$\langle G^R_{il,2}(E+\omega)G^A_{kj,2}(E)\rangle_C =$$
$$\frac{2\pi}{N_2^2\delta_2}\frac{\delta_{ik}\delta_{lj}}{-i\omega}\frac{1+i\sqrt{\xi}\frac{E_U}{\omega}+i\frac{E_{X_1}}{\omega}}{1+i\frac{E_{X_1}+E_{X_2}}{\omega}-\frac{E_{X_1}E_{X_2}}{\omega^2}-\frac{E_{X_1}E_U}{\sqrt{\xi}\omega^2}-\frac{\sqrt{\xi}E_{X_2}E_U}{\omega^2}+i\left(\sqrt{\xi}+\frac{1}{\sqrt{\xi}}\right)\frac{E_U}{\omega}\left(1+i\frac{E_\Gamma}{\omega}\right)}. \tag{B23}$$

Finally, the connected part of the total two-particle Green's function is obtained as a sum of diffuson and cooperon parts, yielding:

$$\langle G^R_{\alpha\gamma,1}(E+\omega)G^A_{\delta\beta,1}(E)\rangle = \frac{2\pi}{N_1^2\delta_1}\frac{\delta_{\alpha\beta}\delta_{\gamma\delta}}{-i\omega}\frac{1+\frac{i}{\sqrt{\xi}}\frac{E_U}{\omega}}{1+i(\sqrt{\xi}+\frac{1}{\sqrt{\xi}})\frac{E_U}{\omega}}+$$
$$\frac{2\pi}{N_1^2\delta_1}\frac{\delta_{\alpha\delta}\delta_{\gamma\beta}}{-i\omega}\frac{1+\frac{i}{\sqrt{\xi}}\frac{E_U}{\omega}+i\frac{E_{X_2}}{\omega}}{1+i\frac{E_{X_1}+E_{X_2}}{\omega}-\frac{E_{X_1}E_{X_2}}{\omega^2}-\frac{E_{X_1}E_U}{\sqrt{\xi}\omega^2}-\frac{\sqrt{\xi}E_{X_2}E_U}{\omega^2}+i\left(\sqrt{\xi}+\frac{1}{\sqrt{\xi}}\right)\frac{E_U}{\omega}\left(1+i\frac{E_\Gamma}{\omega}\right)} \tag{B24}$$

$$\langle G^R_{il,2}(E+\omega)G^A_{kj,2}(E)\rangle = \frac{2\pi}{N_2^2\delta_2}\frac{\delta_{ij}\delta_{lk}}{-i\omega}\frac{1+i\sqrt{\xi}\frac{E_U}{\omega}}{1+i(\sqrt{\xi}+\frac{1}{\sqrt{\xi}})\frac{E_U}{\omega}}+$$
$$\frac{2\pi}{N_2^2\delta_2}\frac{\delta_{ik}\delta_{lj}}{-i\omega}\frac{1+i\sqrt{\xi}\frac{E_U}{\omega}+i\frac{E_{X_1}}{\omega}}{1+i\frac{E_{X_1}+E_{X_2}}{\omega}-\frac{E_{X_1}E_{X_2}}{\omega^2}-\frac{E_{X_1}E_U}{\sqrt{\xi}\omega^2}-\frac{\sqrt{\xi}E_{X_2}E_U}{\omega^2}+i\left(\sqrt{\xi}+\frac{1}{\sqrt{\xi}}\right)\frac{E_U}{\omega}\left(1+i\frac{E_\Gamma}{\omega}\right)}. \tag{B25}$$

APPENDIX C: FOURIER TRANSFORM OF TWO-PARTICLE GREEN'S FUNCTION

To be able to study temporal behavior of electrons in the rmt system we introduce the Fourier transform of two-particle Green's function. We define it via the following integral:

$$\langle G^R_{\alpha\gamma}(t)G^A_{\delta\beta}(t)\rangle = \frac{1}{(2\pi)^2}\int_{-\infty}^{+\infty}\exp^{-i\omega t}\langle G^R_{\alpha\gamma}(E+\omega)G^A_{\delta\beta}(E)\rangle d\omega dE. \tag{C1}$$

To get the correct behavior of the diffuson part for small ω, we replace $1/\omega$ by $\omega/(\omega^2+\eta^2)$, where η is infinitesimal positive number. Now we introduce for dot 1:

$$f_D(\omega) = \frac{2\pi}{N_1^2\delta_1}\frac{\delta_{\alpha\beta}\delta_{\gamma\delta}}{-i\omega}\frac{1+\frac{i}{\sqrt{\xi}}\frac{E_U}{\omega}}{1+i\left(\sqrt{\xi}+\frac{1}{\sqrt{\xi}}\right)\frac{E_U}{\omega}} \to \delta_{\alpha\beta}\delta_{\gamma\delta}\frac{2\pi}{N_1^2\delta_1}\frac{i\omega}{\omega^2+\eta^2}\frac{\omega+\frac{i}{\sqrt{\xi}}E_U}{\omega+i\left(\sqrt{\xi}+\frac{1}{\sqrt{\xi}}\right)E_U}$$
$$= \delta_{\alpha\beta}\delta_{\gamma\delta}\frac{2\pi}{N_1^2\delta_1}\frac{i\omega\left(\omega+\frac{i}{\sqrt{\xi}}E_U\right)}{(\omega-i\eta)(\omega+i\eta)(\omega+i(\sqrt{\xi}+\frac{1}{\sqrt{\xi}})E_U)}. \quad \text{(C2)}$$

The Fourier transform of this diffuson term gives:

$$f_D(t) = \frac{1}{2\pi}\int_{-\infty}^{+\infty}\exp(-i\omega t)f_D(\omega)d\omega. \quad \text{(C3)}$$

Next steps are the standard steps of integration in complex plane. For $t > 0$ one closes contour in lowerhalf plane. One root is located in upper half plane and two more are located in lower half plane. The integration yields:

$$f_D(t) = \delta_{\alpha\beta}\delta_{\gamma\delta}\frac{2\pi}{N_1^2\delta_1}\left[\frac{(\frac{E_U}{\sqrt{\xi}}-\eta)e^{-\eta t}}{2\left((\sqrt{\xi}+\frac{1}{\sqrt{\xi}})E_U-\eta\right)} + \frac{(\sqrt{\xi}+\frac{1}{\sqrt{\xi}})\sqrt{\xi}E_U^2 e^{-(\sqrt{\xi}+\frac{1}{\sqrt{\xi}})E_U t}}{(\sqrt{\xi}+\frac{1}{\sqrt{\xi}})^2E_U^2-\eta^2}\right]. \quad \text{(C4)}$$

As η approaches zero, $f_D(t)$ becomes:

$$f_D(t) = \delta_{\alpha\beta}\delta_{\gamma\delta}\frac{2\pi}{N_1^2\delta_1}\frac{1}{1+\xi}\left[\frac{1}{2}+\xi e^{-(\sqrt{\xi}+\frac{1}{\sqrt{\xi}})E_U t}\right]. \quad \text{(C5)}$$

The full Fourier transformation includes integration over E as well. In current approximation, when E is close to the center of the band, $\langle G_1^R G_1^A\rangle$ is independent of E. It will depend on E if we integrate over the whole bandwidth. The exact dependence of $\langle G_1^R G_1^A\rangle$ on E far from the center of the band is not known. To get correct expression we assume that integration over E adds to $\langle G_1^R G_1^A\rangle$ multiplicative factor $N_1\delta_1$ along with normalization coefficient A. Also, for index pairing $\alpha = \beta$ and $\gamma = \delta$, $G^R_{\alpha\gamma}G^A_{\delta\beta}$ becomes transition probability density $P(t)_{\alpha\to\gamma}$. Using equipartition theorem, for $t \to \infty$ summation of $P(t)_{\alpha\to\gamma}$ over α one can get total probability to stay in dot 1. It is equal to $N_1/(N_1+N_2)$. That is,

$$\sum_\alpha \int dE f_D(t) = \frac{N_1}{N_1+N_2} = \frac{1}{1+\xi}. \quad \text{(C6)}$$

Integration over E and summation over α gives the factor of $AN_1^2\delta_1$. We identify the normalization constant as $A = 1/\pi$. Note, that we did not use cooperon part $f_C(t)$ to

determine normalization constant A. The reason for that is chosen index pairing. After the summation over α cooperon part contribution is of the order $1/N_1$ compared with the diffuson part. After integration over E with proper normalization $f_D(t)$ becomes:

$$f_D(t) = \delta_{\alpha\beta}\delta_{\gamma\delta}\frac{2}{N_1(1+\xi)}\left[\frac{1}{2} + \xi e^{-(\sqrt{\xi}+\frac{1}{\sqrt{\xi}})E_U t}\right]. \tag{C7}$$

Then we perform the Fourier transform of the cooperon part:

$$f_C(\omega) = \frac{2\pi}{N_1^2\delta_1}\frac{\delta_{\alpha\delta}\delta_{\gamma\beta}}{-i\omega}\frac{1 - \frac{E_{X_2}}{i\omega} - \frac{1}{\sqrt{\xi}}\frac{E_U}{i\omega}}{1 - \frac{E_{X_1}+E_{X_2}}{i\omega} + \frac{E_{X_1}E_{X_2}}{(i\omega)^2} + \frac{E_{X_1}E_U}{\sqrt{\xi}(i\omega)^2} + \frac{\sqrt{\xi}E_{X_2}E_U}{(i\omega)^2} + \left(\sqrt{\xi}+\frac{1}{\sqrt{\xi}}\right)\frac{E_U}{i\omega}\left(\frac{E_\Gamma}{i\omega} - 1\right)}. \tag{C8}$$

The $f_C(\omega)$ is a regular function when ω approaches limiting values, provided at least one of the crossover energy scales E_{X_1}, E_{X_2}, or E_Γ differs from zero.

To make $f_C(\omega)$ more suitable for the Fourier transform we manipulate Eq. (C8) into:

$$\begin{aligned} f_C(\omega) = &-\delta_{\alpha\delta}\delta_{\gamma\beta}\frac{2\pi}{N_1^2\delta_1}\left[i\omega - E_{X_2} - \frac{E_U}{\sqrt{\xi}}\right] \\ &\times\left[(i\omega)^2 - \left((E_{X_1}+\sqrt{\xi}E_U) + (E_{X_2}+\frac{E_U}{\sqrt{\xi}})\right)(i\omega)\right. \\ &\left. + \left(E_{X_1}E_{X_2} + \frac{E_{X_1}E_U}{\sqrt{\xi}} + E_{X_2}E_U\sqrt{\xi} + (\sqrt{\xi}+\frac{1}{\sqrt{\xi}})E_U E_\Gamma\right)\right]^{-1}. \end{aligned} \tag{C9}$$

and observe that the poles of $f_C(\omega)$ are given by

$$i\omega_\pm = \frac{(E_{X_1}+\sqrt{\xi}E_U) + (E_{X_2}+\frac{E_U}{\sqrt{\xi}}) \pm \sqrt{\mathfrak{D}}}{2} \tag{C10}$$

with $\mathfrak{D} = ((E_{X_1}+\sqrt{\xi}E_U) - (E_{X_2}+E_U/\sqrt{\xi}))^2 + 4E_U^2(1-4\Gamma^2)$. The parameter $\mathfrak{D}$ is always positive and $\omega_\pm$ are imaginary complex numbers.

It can be proved that $(E_{X_1}+\sqrt{\xi}E_U)+(E_{X_2}+E_U/\sqrt{\xi}) > \sqrt{\mathfrak{D}}$ for all values of parameters, which means that the poles are pure imaginary numbers in lower half complex plane:

$$\omega_\pm = -i\frac{(E_{X_1}+\sqrt{\xi}E_U) + (E_{X_2}+\frac{E_U}{\sqrt{\xi}}) \pm \sqrt{\mathfrak{D}}}{2} = -ia_\pm, \qquad a_+ > a_- > 0. \tag{C11}$$

The function $f_C(\omega)$ now reads:

$$f_C(\omega) = -\delta_{\alpha\delta}\delta_{\gamma\beta}\frac{2\pi}{N_1^2\delta_1}\frac{i\omega - E_{X_2} - \frac{E_U}{\sqrt{\xi}}}{(i\omega - a_-)(i\omega - a_+)}. \tag{C12}$$

We perform the Fourier transform and use the normalization factor to obtain:

$$f_C(t) = \frac{1}{2\pi}\int_{-\infty}^{+\infty} \exp(-i\omega t) f_C(\omega) d\omega dE = \delta_{\alpha\delta}\delta_{\gamma\beta}\frac{2}{N_1}\left[1 + \frac{E_{X_2} + \frac{E_U}{\sqrt{\xi}}}{a_+ - a_-}\left(e^{-ta_-} - e^{-ta_+}\right)\right]. \tag{C13}$$

Hence, the full expression for the Fourier transform for the two-particle Green's function in the dot are given by:

$$\langle G^R_{\alpha\gamma}(t) G^A_{\delta\beta}(t)\rangle_{11} = \delta_{\alpha\beta}\delta_{\delta\gamma}\frac{2}{N_1(1+\xi)}\left[\frac{1}{2} + \xi e^{-(\sqrt{\xi}+\frac{1}{\sqrt{\xi}})E_U t}\right] + \delta_{\alpha\delta}\delta_{\gamma\beta}\frac{2}{N_1}\left[1 + \frac{E_{X_2} + \frac{E_U}{\sqrt{\xi}}}{a_+ - a_-}\left(e^{-ta_-} - e^{-ta_+}\right)\right] \tag{C14}$$

$$\langle G^R_{ik}(t) G^A_{lj}(t)\rangle_{22} = \delta_{ij}\delta_{kl}\frac{2\xi}{N_2(1+\xi)}\left[\frac{1}{2} + \frac{1}{\xi}e^{-(\sqrt{\xi}+\frac{1}{\sqrt{\xi}})E_U t}\right] + \delta_{il}\delta_{kj}\frac{2}{N_2}\left[1 + \frac{E_{X_1} + \sqrt{\xi}E_U}{a_+ - a_-}\left(e^{-ta_-} - e^{-ta_+}\right)\right], \tag{C15}$$

where $a_\pm$ is defined through Eq. (C11).

APPENDIX D: CORRELATION OF FOUR WAVE FUNCTIONS

In this appendix we obtain correlation of four wave functions $\langle \psi_n(\alpha)\psi_n^*(\gamma)\psi_m(\delta)\psi_m^*(\beta)\rangle$ for the system of two coupled dots. This has been obtained in a single dot for the pure ensembles by supersymmetry methods by Mirlin[50], and for the GOE→GUE crossover by Adam *et al*[23]. We consider ensemble average of the following product:

$$\langle \left[G^R_{\alpha\gamma}(E+\omega) - G^A_{\alpha\gamma}(E+\omega)\right]\left[G^R_{\delta\beta}(E) - G^A_{\delta\beta}(E)\right]\rangle \approx$$
$$-\langle G^R_{\alpha\gamma}(E+\omega)G^A_{\delta\beta}(E) - \langle G^A_{\alpha\gamma}(E+\omega)G^R_{\delta\beta}(E)\rangle = -2(\delta_{\alpha\beta}\delta_{\gamma\delta}Re[D_1] + \delta_{\alpha\delta}\delta_{\gamma\beta}Re[C_1]), \tag{D1}$$

where D_1 and C_1 are the diffuson and cooperon expressions from Eq. (27). Here we used the fact that ensemble average of G^RG^R and G^AG^A are smaller than G^RG^A and G^AG^R.

On the other hand, we have:

$$G^R_{\alpha\gamma}(E) - G^A_{\alpha\gamma}(E) = -2\pi i \sum_n \psi_n(\alpha)\psi^*_n(\gamma)\delta(E - E_n), \tag{D2}$$

and

$$\langle \left[G^R_{\alpha\gamma}(E+\omega) - G^A_{\alpha\gamma}(E+\omega)\right]\left[G^R_{\delta\beta}(E) - G^A_{\delta\beta}(E)\right]\rangle \approx$$
$$- 4\pi^2 \langle \sum_{n,m} \psi_n(\alpha)\psi^*_n(\gamma)\psi_m(\delta)\psi^*_m(\beta)\delta(E+\omega-E_n)\delta(E-E_m)\rangle. \tag{D3}$$

We know that in the crossover components of eigenvalues and eigenvectors are correlated with each other. This correlation is small already on the distances of a few δ and can be neglected in the limit $\omega \gg \delta$, so Eq. (D3) can be approximated by:

$$-4\pi^2 \langle \psi_{\bar{n}}(\alpha)\psi^*_{\bar{n}}(\gamma)\psi_{\bar{m}}(\delta)\psi^*_{\bar{n}}(\beta)\rangle \langle \sum_n \delta(E+\omega-E_n)\rangle \langle \sum_m \delta(E-E_m)\rangle.$$

where $\bar{n}$ and $\bar{m}$ mark energy levels close to $E+\omega$ and E respectively.

The average of the sum is a density of states $\rho(E) = \langle \sum_n \delta(E-E_n)\rangle = 1/\delta$. Then, we get

$$\langle \left[G^R_{\alpha\gamma}(E+\omega) - G^A_{\alpha\gamma}(E+\omega)\right]\left[G^R_{\delta\beta}(E) - G^A_{\delta\beta}(E)\right]\rangle \approx$$
$$- \frac{4\pi^2}{\delta^2} \langle \psi_n(\alpha)\psi^*_n(\gamma)\psi_m(\delta)\psi^*_m(\beta)\rangle. \tag{D4}$$

For the two coupled dots we have:

$$Re[D_1] = \frac{2\pi}{N_1\delta_1} \frac{\sqrt{\xi}E_U}{\omega^2 + (\sqrt{\xi} + \frac{1}{\sqrt{\xi}})^2 E_U^2} \tag{D5}$$

In order to calculate $Re[C_1]$ from Eq. (27) we are going to assume that magnetic field is zero in the first dot and in the hopping region ($E_{X_1} = E_\Gamma = 0$), and the second dot is in GOE to GUE crossover ($E_{X_2} \sim \omega$). Then,

$$Re[C_1] = \frac{2\pi}{N_1^2\delta_1} \frac{\sqrt{\xi}E_U\omega^2 + (E_U + \sqrt{\xi}E_{X_2})E_U E_{X_2}}{(\omega^2 - \sqrt{\xi}E_U E_{X_2})^2 + (E_{X_2} + (\sqrt{\xi} + \frac{1}{\sqrt{\xi}})E_U)^2\omega^2} \tag{D6}$$

The relation between the mean level spacing δ for the system of coupled dots and the mean level spacing in the first uncoupled dot δ_1 is as follows. The averaged density of states

in coupled system is going to be the sum of densities of each dot: $\langle\rho\rangle = \langle\rho_1\rangle + \langle\rho_2\rangle$, or $\delta^{-1} = \delta_1^{-1} + \delta_2^{-1}$. Thus, we conclude that $\delta = \delta_1/(1+\xi)$.

Finally, we set Eq. (D1) and Eq. (D4) equal and obtain correlation of for the wave functions:

$$\langle\psi_n(\alpha)\psi_n^*(\gamma)\psi_m(\delta)\psi_m^*(\beta)\rangle = \delta_{\alpha\beta}\delta_{\gamma\delta}\,\frac{\delta_1}{\pi(1+\xi)^2N_1^2}\,\frac{\sqrt{\xi}E_U}{\omega^2+(\sqrt{\xi}+\frac{1}{\sqrt{\xi}})^2E_U^2} + \delta_{\alpha\delta}\delta_{\gamma\beta}\,\frac{\delta_1 E_U}{\pi(1+\xi)^2N_1^2}\,\frac{\sqrt{\xi}\omega^2+(\sqrt{\xi}E_{X_2}^2+E_UE_{X_2})}{(\omega^2-\sqrt{\xi}E_UE_{X_2})^2+(E_{X_2}+(\sqrt{\xi}+\frac{1}{\sqrt{\xi}})E_U)^2\omega^2}. \quad \text{(D7)}$$

APPENDIX E: SUM RULE FOR DOUBLE DOT SYSTEM

To verify the expressions we have obtained for the averaged Green's functions we use a sum rule.

The pair annihilation (creation) operator $T(T^\dagger)$ in the basis of two uncoupled dots is a sum of two terms belonging to each dot:

$$\begin{aligned} T &= \sum_{\alpha_0} c_{\alpha_0,\downarrow}c_{\alpha_0,\uparrow} + \sum_{i_0} c_{i_0,\downarrow}c_{i_0,\uparrow}, \\ T^\dagger &= \sum_{\alpha_0} c^\dagger_{\alpha_0,\uparrow}c^\dagger_{\alpha_0,\downarrow} + \sum_{i_0} c^\dagger_{i_0,\uparrow}c^\dagger_{i_0,\downarrow}. \end{aligned} \quad \text{(E1)}$$

Greek indices go over the states in the first dot, and Latin indices go over the states in the second dot. The subindex 0 denotes the basis of two uncoupled dots.

Our first goal is to calculate the commutator $[T^\dagger, T]$. As operators from different dots anticommute, one gets:

$$[T^\dagger, T] = \sum_{\alpha_0,\beta_0}[c^\dagger_{\alpha_0,\uparrow}c^\dagger_{\alpha_0,\downarrow}, c_{\beta_0,\downarrow}c_{\beta_0,\uparrow}] + \sum_{i_0,j_0}[c^\dagger_{i_0,\uparrow}c^\dagger_{i_0,\downarrow}, c_{j_0,\downarrow}c_{j_0,\uparrow}] = \hat{N}_{1e} + \hat{N}_{2e} - N_1 - N_2, \quad \text{(E2)}$$

where $\hat{N}_{1e}, \hat{N}_{2e}$ are the operators of total number of electrons in dot 1 and dot 2, and N_1, N_2 are the total number of levels in dot 1 and dot 2.

The expectation value of $[T^\dagger, T]$ in ground state at zero temperature is:

$$\overline{[T^\dagger, T]} = \langle\Omega|[T^\dagger, T]|\Omega\rangle = N_e - N. \quad \text{(E3)}$$

N_e and N are the total number of electrons and levels in both dots. This number is conserved when going to another basis.

Now we choose the basis of the system of coupled dots. In this basis $c_{\alpha_0,s} = \sum_m \psi_m(\alpha_0)c_{m,s}$, and $c_{i_0,s} = \sum_m \psi_m(i_0)c_{m,s}$, where $c_{m,s}$ is annihilation operator in new basis. Using this transformation, we rewrite pair destruction operator as follows:

$$T = \sum_{\alpha_0} c_{\alpha_0,\downarrow}c_{\alpha_0,\uparrow} + \sum_{i_0} c_{i_0,\downarrow}c_{i_0,\uparrow} = \sum_{m_1,m_2} D_{m_1m_2}c_{m_1,\downarrow}c_{m_2,\uparrow}, \tag{E4}$$

where $D_{m_1m_2}$ is defined by the following expression:

$$\begin{aligned} D_{m_1m_2} = \sum_{m_1,m_2}\left(\sum_{\alpha_0}\psi_{m_1}(\alpha_0)\psi_{m_2}(\alpha_0) + \sum_{i_0}\psi_{m_1}(i_0)\psi_{m_2}(i_0)\right)c_{m_1,\downarrow}c_{m_2,\uparrow} \\ = \sum_{p_0}\psi_{m_1}(p_0)\psi_{m_2}(p_0). \end{aligned} \tag{E5}$$

The index p_0 runs over all states in the first and second dots for the basis of uncoupled dots.

In the new basis the $T, T^\dagger$ operators look like this:

$$\begin{aligned} T &= \sum_{m_1,m_2} D_{m_1m_2}c_{m_1,\downarrow}c_{m_2,\uparrow}, \\ T^\dagger &= \sum_{m_1,m_2} D^*_{m_1m_2}c^\dagger_{m_2,\uparrow}c^\dagger_{m_1,\downarrow}. \end{aligned} \tag{E6}$$

Consequently, in the new basis,

$$\begin{aligned} [T^\dagger, T] &= \sum_{m_1,m_2}\sum_{m_3,m_4} D^*_{m_1m_2}D_{m_3m_4}[c^\dagger_{m_2,\uparrow}c^\dagger_{m_1,\downarrow}, c_{m_3,\downarrow}c_{m_4,\uparrow}] \\ &= \sum_{m_2,m_4}\left(\sum_{m_1} D^*_{m_1m_2}D_{m_1m_4}\right)c^\dagger_{m_2,\uparrow}c_{m_4,\uparrow} - \sum_{m_1,m_3}\left(\sum_{m_2} D^*_{m_1m_2}D_{m_3m_2}\right)c_{m_3,\downarrow}c^\dagger_{m_1,\downarrow}. \end{aligned} \tag{E7}$$

One can go further and use completeness condition $\sum_m \psi^*_m(p_0)\psi_m(n_0) = \delta_{p_0n_0}$ to show that in the new basis the value of commutator is $\hat{N}_e - N$. Our next goal, however, is to take the disorder average of the vacuum expectation value and to prove the invariance of $[T^\dagger, T]$.

Taking into account that $\langle\Omega|c^\dagger_{m_1,\uparrow}c_{m_2,\uparrow}|\Omega\rangle = \delta_{m_1m_2}\Theta(\mu - E_{m_1})$ and $\langle\Omega|c_{m_2,\downarrow}c^\dagger_{m_1,\downarrow}|\Omega\rangle = \delta_{m_1m_2}(1 - \Theta(\mu - E_{m_1}))$, the ground state expectation value for the commutator is:

$$\overline{[T^\dagger, T]} = \langle\Omega|[T^\dagger, T]|\Omega\rangle = \sum_{m_1,m_2} |D_{m_1m_2}|^2[2\Theta(\mu - E_{m_1}) - 1], \tag{E8}$$

where $\Theta(x)$ is a step function.

Averaging over disorder gives:

$$\langle\overline{[T^\dagger, T]}\rangle = 2\sum_{m_1,m_2} \Theta(\mu - E_{m_1})\langle|D_{m_1m_2}|^2\rangle - \sum_{m_1,m_2} \langle|D_{m_1m_2}|^2\rangle \tag{E9}$$

Converting this into integral, we get:

$$\langle\overline{[T^\dagger, T]}\rangle = 2\int_{-W}^{\mu}\int_{-W}^{W} dE_1dE_2\rho(E_1)\rho(E_2)\langle|D(E_1, E_2)|^2\rangle - \int_{-W}^{W}\int_{-W}^{W} dE_1dE_2\rho(E_1)\rho(E_2)\langle|D(E_1, E_2)|^2\rangle \tag{E10}$$

The density of states $\rho(E)$ is the Winger's semicircle law:

$$\rho(E) = \frac{2N}{\pi W^2}\sqrt{W^2 - E^2},$$

where $2W$ is the bandwidth and N is the number of states in the system.

To proceed we need to find the ensemble average of the following object:

$$\langle|D_{m_1m_2}|^2\rangle = \sum_{p_0,n_0}\langle\psi^*_{m_1}(p_0)\psi^*_{m_2}(p_0)\psi_{m_1}(n_0)\psi_{m_2}(n_0)\rangle. \tag{E11}$$

Using results of appendix D one can obtain expression for the correlation of four wave functions in the form:

$$\langle\psi^*_{m_1}(p_0)\psi^*_{m_2}(p_0)\psi_{m_1}(n_0)\psi_{m_2}(n_0)\rangle = \frac{1}{2\pi^2\rho(E_1)\rho(E_2)} Re\Big[\sum_{p_0n_0}\langle G^R_{n_0p_0}(E_2)G^A_{n_0p_0}(E_1)\rangle - \sum_{p_0n_0}\langle G^R_{n_0p_0}(E_2)G^R_{n_0p_0}(E_1)\rangle\Big]. \tag{E12}$$

Note, that to get the correct answer for the sum rule one should keep $\langle G^R G^R\rangle$ term as well. Summation in Eq. (E12) is performed over the states in both dots.

When the dots have equal mean level spacing $\delta_1 = \delta_2 = \delta_0$, one particle Green's function can be found exactly from the system (B7) without approximation in U:

$$\langle G^R_{p_0 p_0'}(E)\rangle = \frac{\delta_{p_0 p_0'}}{\frac{E}{2}+\frac{i}{2}\sqrt{W^2-E^2}} = -\frac{2i}{W}e^{i\phi}$$
$$\langle G^A_{p_0 p_0'}(E)\rangle = \frac{\delta_{p_0 p_0'}}{\frac{E}{2}-\frac{i}{2}\sqrt{W^2-E^2}} = \frac{2i}{W}e^{-i\phi}, \tag{E13}$$

where $W = 2N_0\delta_0\sqrt{1+U}/\pi$ is the half bandwidth and $\sin\phi = E/W$. Here both indices p_0 and p_0' belong either to the first or to the second dot.

The sum in Eq. (E12) can be broken into four sums, when the indices p_0, n_0 belong either to the first dot, or to the second dot, or one of the indices go over the states in the first dot, and the other one goes over the states in the second dot.

For example, for $\langle G^R G^A\rangle$ part we have the following expression:

$$\sum_{p_0 n_0}\langle G^R_{n_0 p_0}(E_2) G^A_{n_0 p_0}(E_1)\rangle =$$
$$N_0\left(\frac{2}{W}\right)^2(1+U)\frac{(1+U)e^{-i\phi_{21}}-\zeta}{[(1+U)e^{-i\phi_{21}}-1][(1+U)e^{-i\phi_{21}}-\zeta]-U^2}$$
$$+N_0\left(\frac{2}{W}\right)^2(1+U)\frac{(1+U)e^{-i\phi_{21}}-1}{[(1+U)e^{-i\phi_{21}}-1][(1+U)e^{-i\phi_{21}}-\zeta]-U^2} \tag{E14}$$
$$+2N_0\left(\frac{2}{W}\right)^2(1+U)\frac{U}{[(1+U)e^{-i\phi_{21}}-1][(1+U)e^{-i\phi_{21}}-\zeta]-U^2}.$$

Here $\phi_{21} = \phi_2 - \phi_1$, and $\zeta = (1-X_2^2)/(1+X_2^2)$

The first term in Eq. (E14) is the contribution of $\langle G^R\rangle\langle G^A\rangle$ plus the cooperon part of two particle Green's function in the first dot. The second term describes contribution of free term and cooperon part in the second dot. The last term is a sum of transition parts from dot 1 to dot 2 and vice versa. It appears that these transition terms are equal, which explains coefficient 2 in front of the last term in Eq. (E14).

Summation of the $\langle G^R G^R\rangle$ gives similar result:

$$\sum_{p_0 n_0} \langle G^R_{n_0 p_0}(E_2) G^R_{n_0 p_0}(E_1)\rangle =$$

$$\begin{aligned} &-N_0 \left(\frac{2}{W}\right)^2 (1+U) \frac{(1+U)e^{-i\psi_{21}} + \zeta}{[(1+U)e^{-i\psi_{21}}+1][(1+U)e^{-i\psi_{21}}+\zeta] - U^2} \\ &-N_0 \left(\frac{2}{W}\right)^2 (1+U) \frac{(1+U)e^{-i\psi_{21}} + 1}{[(1+U)e^{-i\psi_{21}}+1][(1+U)e^{-i\psi_{21}}+\zeta] - U^2} \\ &+2N_0 \left(\frac{2}{W}\right)^2 (1+U) \frac{U}{[(1+U)e^{-i\psi_{21}}+1][(1+U)e^{-i\psi_{21}}+\zeta] - U^2}, \end{aligned} \tag{E15}$$

where $\psi_{21} = \phi_2 + \phi_1$.

In principle, there should be terms corresponding to diffusons in dot 1 and dot 2. However, these terms after summation over p_0, n_0 are $1/N_0$ smaller than the others and in the large N_0 limit can be neglected.

Although one can use Eq. (E10) to verify the sum rule, it is more convenient to work with derivative of Eq. (E10) over μ at $\mu = 0$.

It gives:

$$\frac{\partial}{\partial \mu} \langle \overline{[T^\dagger, T]} \rangle_{\mu=0} = 2\rho(0) \int_{-W}^{W} dE_2 \rho(E_2) \langle |D(E_1 = 0, E_2)|^2 \rangle. \tag{E16}$$

On the other hand, this expression should be equal to:

$$\frac{\partial}{\partial \mu}(N_e - N) = \frac{\partial}{\partial \mu}\big(2\frac{N}{2} + 2\int_0^\mu \rho(E) dE - N\big) = 2\rho(\mu). \tag{E17}$$

Comparison of Eq. (E16) and (E17) at $\mu = 0$ results in the following condition for the sum rule:

$$\int_{-W}^{W} dE_2 \rho(E_2) \langle |D(E_1 = 0, E_2)|^2 \rangle = 1. \tag{E18}$$

The integral in Eq. (E18) was computed numerically and matched the unity with high accuracy.

---

* Electronic address: zelyak@pa.uky.edu

† Electronic address: murthy@pa.uky.edu

‡ Electronic address: rozhkois@notes.udayton.edu

[1] E. Wigner, Ann. Math. **62**, 548 (1955).

[2] E. Wigner, Ann. Math. **65**, 203 (1957).

[3] M. L. Mehta, *Random Matrices*, vol. 142 of *Pure and Applied Mathematics* (Academic Press, 2004), 3rd ed.

[4] L. Gorkov and G. Eliashberg, Zh. Eksp. i Teor. Fiz. **48**, 1407 (1965).

[5] B. L. Al'tshuler and B. I. Shklovskii, Sov. Phys. JETP **64**, 127 (1986).

[6] K. Efetov, Advances in Physics **32**, 53 (1983).

[7] O. Bohigas, M. J. Giannoni, and C. Schmit, Phys. Rev. Lett. **52**, 1 (1984).

[8] A. Hönig and D. Wintgen, Phys. Rev. A **39**, 5642 (1989).

[9] T. Zimmermann, H. Köppel, L. S. Cederbaum, G. Persch, and W. Demtröder, Phys. Rev. Lett. **61**, 3 (1988).

[10] S. Deus, P. M. Koch, and L. Sirko, Phys. Rev. E **52**, 1146 (1995).

[11] H.-J. Sommers and S. Iida, Phys. Rev. E **49**, R2513 (1994).

[12] I. L. Aleiner, P. W. Brouwer, and L. I. Glazman, Phys. Rep. **358**, 309 (2002).

[13] A. Altland, Y. Gefen, and G. Montambaux, Phys. Rev. Lett. **76**, 1130 (1996).

[14] K. Efetov, *Supersymmetry in Disorder and Chaos* (Cambridge University Press, 1999).

[15] A. Abrikosov, *Methods of Quantum Field Theory in Statistical Physics* (Dover Publications, 1975).

[16] F. R. Waugh, M. J. Berry, D. J. Mar, R. M. Westervelt, K. L. Campman, and A. C. Gossard, Phys. Rev. Lett. **75**, 705 (1995).

[17] R. L. Weaver and O. I. Lobkis, Journal of Sound and Vibration **231**, 1111 (2000).

[18] A. Tschersich and K. B. Efetov, Phys. Rev. E **62**, 2042 (2000).

[19] V. I. Fal'ko and K. Efetov, Phys. Rev. B **50**, 11267 (1994).

[20] A. P. J. B. French, V. K. B. Kota and S. Tomsovic, Annals of Physics **181**, 177 (1988).

[21] S. A. van Langen, P. W. Brouwer, and C. W. J. Beenakker, Phys. Rev. E **55**, R1 (1997).

[22] A. Pandey and M. L. Mehta, Communications in Mathematical Physics **87**, 449 (1983).

[23] S. Adam, P. W. Brouwer, J. P. Sethna, and X. Waintal, Phys. Rev. B **66**, 165310 (2002).

[24] S. Adam, P. W. Brouwer, and P. Sharma, Phys. Rev. B **68**, 241311 (2003).

[25] Y. Alhassid and T. Rupp, cond-mat/0312691 (2003).

[26] G. Murthy, Physical Review B (Condensed Matter and Materials Physics) **70**, 153304 (pages 4) (2004).

[27] A. V. Andreev and A. Kamenev, Phys. Rev. Lett. **81**, 3199 (1998).

[28] P. W. Brouwer, Y. Oreg, and B. I. Halperin, Phys. Rev. B **60**, R13977 (1999).

[29] H. U. Baranger, D. Ullmo, and L. I. Glazman, Phys. Rev. B **61**, R2425 (2000).

[30] I. L. Kurland, I. L. Aleiner, and B. L. Altshuler, Phys. Rev. B **62**, 14886 (2000).

[31] G. Murthy and H. Mathur, Phys. Rev. Lett. **89**, 126804 (2002).

[32] G. Murthy and R. Shankar, Phys. Rev. Lett. **90**, 066801 (2003).

[33] G. Murthy, R. Shankar, D. Herman, and H. Mathur, Physical Review B (Condensed Matter and Materials Physics) **69**, 075321 (2004).

[34] R. Shankar, Rev. Mod. Phys. **66**, 129 (1994).

[35] R. Shankar, Physica A: Statistical and Theoretical Physics **177**, 530 (1991).

[36] S. Chakravarty, B. I. Halperin, and D. R. Nelson, Phys. Rev. B **39**, 2344 (1989).

[37] S. Chakravarty, B. I. Halperin, and D. R. Nelson, Phys. Rev. Lett. **60**, 1057 (1988).

[38] S. Sachdev, *Quantum Phase Transitions* (Cambridge University Press, 2001).

[39] A. Kamenev and Y. Gefen, Phys. Rev. B **54**, 5428 (1996).

[40] K. B. Efetov and A. Tschersich, Phys. Rev. B **67**, 174205 (2003).

[41] I. S. Beloborodov, K. B. Efetov, A. V. Lopatin, and V. M. Vinokur, arXiv:cond-mat/0603522 (2006).

[42] L. G. Aslamazov and A. I. Larkin, Sov. Phys. Solis State **10**, 875 (1968).

[43] A. Altland and M. R. Zirnbauer, Phys. Rev. B **55**, 1142 (1997).

[44] A. Altland, B. D. Simons, and M. R. Zirnbauer, Physics Reports **359**, 283 (2002).

[45] M. Schechter, Y. Oreg, Y. Imry, and Y. Levinson, Phys. Rev. Lett. **90**, 026805 (2003).

[46] V. Ambegaokar and U. Eckern, Phys. Rev. Lett. **65**, 381 (1990).

[47] V. Ambegaokar and U. Eckern, Europhysics Letters **13**, 733 (1990).

[48] Y. Alhassid, L. Fang, and S. Schmidt, arXiv:cond-mat/0702304 (2006).

[49] B. L. Altshuler, Y. Gefen, and Y. Imry, Phys. Rev. Lett. **66**, 88 (1991).

[50] A. D. Mirlin, Physics Reports **326**, 259 (2000), URL `http://www.sciencedirect.com/science/article/B6TVP-3YS34MM-2/2/6c0cda8b40b326b5efc838cdd723`

[51] I. L. Aleiner and V. I. Fal'ko, Phys. Rev. Lett. **87**, 256801 (2001).

[52] I. L. Aleiner and V. I. Fal'ko, Phys. Rev. Lett. **89**, 079902 (2002).

[53] G. Dresselhaus, Phys. Rev. **100**, 580 (1955).

[54] Y. Bychkov and E. Rashba, JETP Lett. **39**, 78 (1984).

[55] H.-J. Stöckmann, *Quantum Chaos: An Introduction* (Cambridge University Press, 1999).

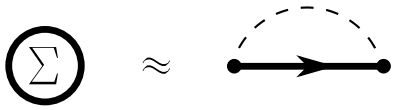
Σ
≈